Fisheries and Oceans Canada | Pêches et Océans Canada
Science | Sciences

Canadian Science Advisory Secretariat (CSAS)

Research Document 2014/049

Québec Region

Chemical and Biological Oceanographic Conditions in the Estuary and Gulf of St. Lawrence during 2011 and 2012

S. Plourde, M. Starr, L. Devine, J.-F. St-Pierre, L. St-Amand, P. Joly, and P. S. Galbraith

Fisheries and Oceans Canada, Québec Region
Maurice Lamontagne Institute
850 de la Mer, P. O. Box 1000
Mont-Joli, QC G5H 3Z4

September 2014

Canada

Foreword

This series documents the scientific basis for the evaluation of aquatic resources and ecosystems in Canada. As such, it addresses the issues of the day in the time frames required and the documents it contains are not intended as definitive statements on the subjects addressed but rather as progress reports on ongoing investigations.

Research documents are produced in the official language in which they are provided to the Secretariat.

Published by:

Fisheries and Oceans Canada
Canadian Science Advisory Secretariat
200 Kent Street
Ottawa ON K1A 0E6

http://www.dfo-mpo.gc.ca/csas-sccs/
csas-sccs@dfo-mpo.gc.ca

ISSN 1919-5044

Correct citation for this publication:

S. Plourde, Starr, M., Devine, L., St-Pierre, J.-F., St-Amand, L., Joly, P., and Galbraith, P. S. 2014. Chemical and biological oceanographic conditions in the Estuary and Gulf of St. Lawrence during 2011 and 2012. DFO Can. Sci. Advis. Sec. Res. Doc. 2014/049. v + 46 pp.

TABLE OF CONTENTS

ABSTRACT iv
RÉSUMÉ v
INTRODUCTION 1
METHODS 1
RESULTS 4
Nutrients and phytoplankton 4
Fixed stations 4
Sections and late-winter helicopter survey 5
Remote sensing of ocean colour 6
Zooplankton 7
Fixed stations 7
Sections 8
Copepod phenology 9
Scorecards 9
DISCUSSION 10
SUMMARY 13
ACKNOWLEDGEMENTS 14
REFERENCES 14

ABSTRACT

This document reports on the chemical and biological conditions in the Gulf of St. Lawrence (GSL) for 2011 and 2012 in the context of a strong warming event that began in 2008. Data from these two years are compared to time-series observations starting in 1999. Zooplankton indices and the spatial scales considered were modified from previous reports to match more closely those of other regions involved in the Atlantic Zone Monitoring Program (AZMP). All phytoplankton and zooplankton abundance indices and nutrient inventories were relatively coherent through the time series (1999–2012) among fixed stations, sections, and large subregions. Winter, spring, and fall surface nitrate inventories have been below the normal since 2010 in many regions of the Gulf. A shift to earlier timing of the spring bloom has also been observed since 2010 across many of the Gulf subregions. In addition, chlorophyll levels during late spring, summer, and fall have tended to be predominately below normal since 2010. There is evidence of ontogenetic and phenological changes in *Calanus* species that appear to be the direct effects of the warmer environmental conditions experienced by the region over the last few years. High abundances of large-bodied arctic and subarctic species occurring simultaneously with the near-record high surface temperature in 2012 suggest that these species avoid or adapt their life cycle strategy to minimize potential negative effects of warm conditions in the surface layer. At the same time, an increased abundance of warm-water species was observed. High abundances of cold/arctic species concomitant with those of warm-water species likely reflect the complex hydrography of the GSL system and highlight the Gulf's position as a transitional zone between the "upstream" Labrador/Newfoundland shelf and the "downstream" Scotian Shelf.

Conditions océanographiques chimiques et biologiques dans l'estuaire et le golfe du Saint-Laurent en 2011 et 2012

RÉSUMÉ

Ce rapport documente les résultats concernant les conditions biologiques dans de golfe du St-Laurent en 2011 et 2012 dans le contexte d'un réchauffement significatif des températures débuté en 2008. Les données de 2011 et 2012 sont comparées à celles de la série temporelle commencée en 1999. Les indices du zooplancton ainsi que les échelles spatiales utilisées ont été modifiés afin de mieux refléter la structure des autres rapports du Programme de Monitorage zonal atlantique (PMZA) des autres régions. Tous les indices de nutriments et d'abondance du phytoplancton et zooplancton pour les stations fixes, les transects et les grandes régions sont cohérents tout le long de la série temporelle (1999–2012). Les niveaux de nitrate en surface au cours de l'hiver, du printemps et de l'automne tendent être en dessous de la normale depuis 2010 dans de nombreuses régions du Golfe du Saint-Laurent. Un changement à la précocité de la floraison printanière est aussi évident dans plusieurs sous-régions du golfe du Saint-Laurent depuis 2010. De plus, les concentrations de chlorophylle à la fin du printemps, au cours de l'été et de l'automne ont tendance à être essentiellement en dessous de la normale depuis 2010. On observe aussi des changements clairs dans l'ontogénie et la phénologie des espèces de *Calanus* qui semblent être causées par des conditions environnementales se réchauffant dans la région depuis quelques années. Les abondances élevées des espèces de gros copépodes arctiques et subarctiques observées simultanément suggèrent que ces espèces pourraient adapter leur stratégie de cycle de vie afin de minimiser les effets négatifs de conditions plus chaudes dans les eaux de surface. Dans le même temps, une augmentation de l'abondance des espèces d'eaux chaudes a été observée. La présence simultanée d'espèces d'eaux froides et d'eaux chaudes reflète la complexité hydrographique du golfe du St-Laurent et montre que ce dernier est positionné comme une zone de transition entre les eaux nordiques du Labrador/Terre Neuve et les eaux plus chaudes du plateau néo-écossais.

INTRODUCTION

The Atlantic Zone Monitoring Program (AZMP) was implemented in 1998 (Therriault et al. 1998) with the aim of (1) increasing the Department of Fisheries and Oceans' (DFO's) capacity to understand, describe, and forecast the state of the marine ecosystem and (2) quantifying the changes in the ocean's physical, chemical, and biological properties and the predator–prey relationships of marine resources. A critical element in the observational program of AZMP is an annual assessment of the distribution and variability of nutrients and the plankton they support.

A description of the spatiotemporal distribution of nutrients (nitrate, silicate, phosphate) and oxygen dissolved in seawater provides important information on water-mass movements and on the locations, timing, and magnitude of biological production cycles. A description of the distribution of phytoplankton and zooplankton provides important information on the organisms forming the base of the marine food web. An understanding of plankton production cycles is an essential part of an ecosystem approach to fisheries management.

The AZMP derives its information on the state of the marine ecosystem from data collected at a network of sampling locations (fixed-point stations, cross-shelf sections) in each DFO region (Québec, Gulf, Maritimes, Newfoundland; see Fig. 1 for Québec and Gulf region locations) sampled at a frequency of twice-monthly to once annually. The sampling design provides basic information on the natural variability in physical, chemical, and biological properties of the Northwest Atlantic continental shelf. Cross-shelf sections provide detailed geographic information but are limited in their seasonal coverage. Critically placed fixed stations complement the geography-based sampling by providing more detailed information on temporal (seasonal) changes in ecosystem properties.

In this document, we review the chemical and biological oceanographic (lower trophic levels) conditions in the Québec region in 2011 and 2012. During these years, surface water temperature and other physical indices showed strong anomalies indicative of a much warmer environment than during the previous decade (Galbraith et al. 2013). In particular, 2012 was characterized by record-high surface temperatures from mid-summer to fall and a strong positive deep-water temperature anomaly. In addition, we saw near-historical values in the cold intermediate layer (CIL; low volume / high minimum temperature index) and in ice conditions (low volume and duration) (Galbraith et al. 2013). Water temperatures were also at record or near-record highs in the other AZMP regions (DFO 2013). In the context of these unusually warm conditions in 2011 and 2012, this report aims to describe changes in the annual production cycles and community composition of phytoplankton and zooplankton.

METHODS

All sample collection and processing steps meet and often exceed the standards of the AZMP protocol (Mitchell et al. 2002). All data included in this report were collected along seven sections during the missions in June and October–November of each year and at the four fixed stations (Fig. 1). Table 1 and Figure 2 show the 2011 and 2012 missions and fixed stations sampling frequencies, respectively. The Gaspé Current (GC), Anticosti Gyre (AG), and Shediac Valley fixed stations were visited less frequently than planned in 2011 and 2012 (Table 1, Fig. 2), while Rimouski station was sampled at roughly weekly intervals from early spring to late fall. The low sampling frequency at GC and AG is the result of a lack of vessel availability, particularly in winter.

Additional sampling was accomplished during a survey of the winter surface mixed layer of the Gulf of St. Lawrence (GSL) and of the surface nutrients (2 m); this survey has taken place in

early to mid-March since 1996 (2002 for nutrients) using a Canadian Coast Guard helicopter. This has added a considerable amount of data to the previously very sparse winter sampling in the region. The survey and sampling methods are described in Galbraith (2006) and in Galbraith et al. (2006). A total of 93 stations were sampled during the 8–17 March 2011 survey and 106 during the 5–17 March 2012 survey. The temperature and salinity of the 2011 and 2012 mixed layers are described by Galbraith et al. (2012, 2013).

Near-surface phytoplankton biomass was estimated from ocean colour data collected by the Sea-viewing Wide Field-of-view Sensor (SeaWiFS) satellite launched by NASA in late summer 1997 and by the Moderate Resolution Imaging Spectroradiometer (MODIS) "Aqua" sensor launched by NASA in July 2002. Because the SeaWIFS mission ended in December 2010, we present here the MODIS data obtained continuously from January 2003 until December 2012 to construct composite time series of surface chlorophyll *a* in six GSL subregions (Anticosti Gyre, Magdalen Shallows, Shediac Valley, Cabot Strait, northwest and northeast Gulf of St. Lawrence; see Fig. 3 for locations). Because data for the estuarine portion of the Gulf are unreliable (due to turbidity and riverine input of terrestrially derived coloured matter), we selected subregions outside of the St. Lawrence River plume. Composite satellite images were created by BIO's remote sensing unit (DFO, Dartmouth, NS) in collaboration with NASA GSFC. Basic statistics (mean, range, standard deviation) are extracted from two-week average composites with a 1.5 km spatial resolution. Seven different metrics were computed using satellite composite data: the timing of spring bloom start and peak (day of year); the magnitude of the spring bloom (maximum chlorophyll *a*); and the chlorophyll *a* mean during spring (March to May), summer (June to August), and fall (September to December) as well as the annual average (March to December). In addition, we computed normalized annual anomalies (see below) for each of the different bloom metrics to evaluate evidence of temporal trends among the different statistical subregions.

Chlorophyll and nutrient data collected along the AZMP sections and at fixed stations were integrated over various depth intervals (i.e., 0–10 m for chlorophyll; 0–5 m and 50–15 m for nutrients) using trapezoidal numerical integration. The surface (0 m) data were actually the shallowest sampled values; data at the lower depths were taken as either i) the interpolated value when sampling was below the lower integration limit or ii) the closest deep-water sampled value when sampling was shallower than the lower integration limit. Integrated nitrate values from the helicopter survey were calculated using surface concentrations (2 m) × 50 m (assuming that the nitrate concentrations are homogeneous in the winter mixed layer at that time of the year).

Some zooplankton data collected in 2000 and 2001 along the AZMP sections and fixed stations were excluded from the present analysis because of serious doubts about the quality of the analysis (they are being re-analyzed in 2013–2014). In this document, the detailed description of seasonal patterns in zooplankton indices was restricted to the Rimouski and Shediac fixed stations due to the very low sampling frequency at GC and AG in 2011 and 2012 (Table 1). However, data from these sites were included in figures to allow comparisons of the seasonal climatology observed at each site and to complement some observations. Finally, we present the seasonal climatologies of zooplankton biomass and total copepodite abundance of *Calanus finmarchicus* and *C. hyperboreus* at Rimouski station for two depth layers (0–100 m, 100–320 m) from 2005 to 2010 (see Perrin et al. 2014 for the methodology) to assess the significance of the fixed sites in quantifying different components of the zooplankton community.

Compared to previous research documents reporting on conditions in the GSL, the number and type of zooplankton indices as well as the way they are reported have been rationalized as a first step toward standardization with research documents from other AZMP regions. We restricted the presentation of results from the fixed sites to total zooplankton biomass, total

copepod abundance, relative contribution of the 10 most abundant copepod species, and *C. finmarchicus* and *Pseudocalanus* spp. abundance and stage composition. Because of its importance to the total zooplankton biomass in the region, a detailed description of *C. hyperboreus* was added. Total zooplankton biomass is the only index presented for the seven standard GSL AZMP sections. We also wished to report GSL results at a spatial scale similar to that used in other regions, so the annual averaged total zooplankton biomass and total abundance of *C. finmarchicus*, *C. hyperboreus,* and *Pseudocalanus* spp. were calculated for three regions having distinct oceanographic regimes (Koutitonsky and Budgen 1991, Galbraith et al. 2013):

- western GSL (wGSL): this region is generally deep (> 200 m) and cold in summer. It is strongly influenced by freshwater runoff from the St. Lawrence River. The wGSL includes the TESL, TSI, and TASO sections.
- southern GSL (sGSL): this region is shallow (< 100 m) and much warmer in summer. It is under the influence of the Gaspé Current. The sGSL includes the TIDM section.
- eastern GSL (eGSL): this region, with deep channels and a relatively wide shelf (< 100 m), is characterized by higher surface salinity and is directly influenced by the intrusion of water from the Labrador and Newfoundland shelves. The eGSL includes the TDC, TCEN, and TBB sections.

These large regions of the GSL correspond more to the scale addressed by AZMP in other regions, where sampling on each section generally targets specific subregions (e.g., Grand Banks, eastern and western Scotian Shelf).

Standardized anomalies of key chemical and biological indices were computed for all fixed stations, sections, and oceanographic regions. These anomalies are calculated as the difference between the variable's average (for the season or for the complete year) and the variable's average for the reference period (usually 1999–2010); this number is then divided by the reference period's standard deviation. These anomalies thus represent observations in a compact format. A standard set of indices representing anomalies of nutrient availability, phytoplankton biomass and bloom dynamics, and the abundance of dominant copepod species and groups (*C. finmarchicus, Pseudocalanus* spp., total copepods, and total non-copepods) are produced for each AZMP region (see DFO 2013). In the present paper, several new zooplankton indices were also computed that reflect either different functional groups with different roles in the ecosystem or groups of species indicative of cold- or warm-water intrusions and/or local environmental conditions: large calanoids (dominated by *Calanus* and *Metridia* species), small calanoids (dominated by more neritic species such as *Centropages* spp., *Pseudocalanus* spp., *Acartia* spp., *Temora* spp.), cyclopoids (dominated by *Oithona* spp. and *Triconia* spp.), warm-water species (*Centropages* spp., *Paracalanus* spp., *Clausocalanus* spp.), and cold/arctic species (*Calanus glacialis*, *Metridia longa*).

Potential changes in zooplankton phenology were also explored using *C. finmarchicus* as an indicator. We used the time series at Rimouski station because adequate sampling and stage identification started there almost 20 years ago (1994). From 1994 to 2004, *C. finmarchicus* copepodite stage abundance was determined using samples collected with 333 µm (CIV–CVI) and 73 µm (CI–III) mesh nets that were analyzed for seven years of the time series (see Plourde et al. 2009 for details). In other years before 2004 for which 73 µm samples were not analyzed, the abundance of CI–III in the 333 µm samples was adjusted based on a comparison

done with an AZMP-like net (S. Plourde, unpublished data[1]). The phenology of *C. finmarchicus* was described using the relative stage proportions of CI–III, CIV, CV, and CVI (male and female). Because the maximum contribution of each stage is not equivalent, with CI–III and CVI typically representing less than 50% of total abundance while CV could be > 90% during fall, we optimized data presentation by using a common scale created by normalizing the relative proportion of each stage: each observation was divided by its observed annual maximum (x/x_{max}).

RESULTS

NUTRIENTS AND PHYTOPLANKTON

Distributions of the primary dissolved inorganic nutrients (nitrate, silicate, phosphate) included in AZMP's observational program strongly co-vary in space and time (Brickman and Petrie 2003). For this reason and because the availability of nitrogen is most often associated with phytoplankton growth limitation in coastal waters of the GSL, emphasis in this document is placed on variability in nitrate concentrations and inventories.

Fixed stations

The Rimouski and Shediac Valley stations typically exhibit a biologically mediated reduction in surface nitrate concentrations in spring/summer, a minimum during summer, and a subsequent increase during fall/winter (Fig. 4). The onset of the nutrient draw-down occurs later at Rimouski station compared to Shediac Valley, reflecting the later spring bloom in the St. Lawrence Estuary (June) compared to Shediac Valley (April). In contrast to Shediac Valley, surface nutrient inventories at Rimouski remain relatively high during summer and usually at levels non-limiting for phytoplankton growth. These high levels are mainly due to upwelling at the head of the Laurentian Channel and the high tidal mixing in this area, and to some degree to anthropogenic and river sources, notably from St. Lawrence River.

At Rimouski station, the onset of spring nutrient draw-down in 2011 and 2012 was similar to the climatological timing (Fig. 4). Spring, summer, and fall inventories at this station were slightly lower than normal in 2011 but close to the long-term average in 2012. Bloom initiation occurred near the average in 2011 but was somewhat later in 2012. Chlorophyll inventories were especially higher than average in June 2011 and 2012, and an intense fall bloom was observed in September 2012. When averaged for the entire sampling period, the chlorophyll inventories were nevertheless close to (2011) or only slightly higher than (2012) the 1999–2010 average.

The seasonal changes in phytoplankton biomass at Shediac Valley in 2011 and 2012 followed the usual pattern of high values during the spring (April–May) and low ones thereafter (Fig. 4). Because of the presence of ice in the Southern Gulf in the spring, only the later phase of the spring bloom is normally caught (as in 2012), or the bloom is completely missed (as in 2011) (Fig. 4); this is evident by the low surface nitrate inventories observed at the start of sampling. Chlorophyll concentrations were nevertheless above the average in April 2012. During the late spring, summer, and fall in both 2011 and 2012, chlorophyll levels were overall below (2011) or close to (2012) the 1999–2010 average.

[1] Fisheries and Oceans Canada, Maurice Lamontagne Institute, 850 route de la Mer, Mont-Joli (QC), G5H 3Z4

In agreement with the chlorophyll data, surface (0–50 m) nitrate inventories at Shediac station in May 2011 and April–May 2012 were well below those observed during the Helicopter survey in March due to utilization by phytoplankton (Fig. 4). Low surface values persisted throughout the summer in 2011 and 2012, and concentrations did not increase again until late fall, as has been previously observed. Compared to the 1999–2010 reference period, surface nutrient inventories were overall well below (2011) or close to (2012) the average.

In 2011 and 2012, diatom, dinoflagellate, and flagellate abundances were below the long-term average at Rimouski station (Fig. 5). While the phytoplankton community was regularly dominated by diatoms throughout the sampling period between 1999 and 2003, a shift from diatoms towards flagellates and dinoflagellates has been observed since 2004 (Fig. 6). The predominance of flagellates and dinoflagellates was nevertheless less pronounced in 2011 and 2012 compared to previous years: the diatom/flagellate and diatom/dinoflagellate ratios were close to the 1999–2010 reference period averages (Fig. 5).

Diatom, dinoflagellate, and flagellate abundances at Shediac station were also below the long-term averages except in 2011, when flagellate abundance was well above normal (Fig. 7). The seasonal evolution of the phytoplankton community composition at Shediac Valley station in 2011 and 2012 was broadly similar to that seen previously, i.e., diatoms dominated during the spring bloom, with >75% of the total count, while flagellates and dinoflagellates dominated (>60% of the total count) summer (Fig. 6). However, flagellates had a higher relative abundance in 2012 than usual during fall. In addition, the time-series anomalies revealed that the diatom/flagellate ratio at the Shediac Valley station has tended to be predominately below normal since 2009, as was observed for the Rimouski station.

Sections and late-winter helicopter survey

In 2011 and 2012, late winter nitrate inventories were relatively high at the surface for most regions of the GSL except for unusually low (<2 mmol m^{-3}) concentrations at some stations in the southern GSL in 2012 (Fig. 8). These atypical low levels in the southern GSL are probably due to an unusual localized start of phytoplankton growth at that time of the year; this is also seen in the satellite ocean colour data (see below). A similar phenomenon was observed in 2010 that caused strong negative anomalies in the northwestern and southern GSL (Fig. 9). In 2011 and 2012, the highest winter surface nitrate concentrations were observed in the St. Lawrence Estuary (SLE), and these values reached minima toward Cabot Strait and in the northeastern GSL, as in previous years. Transport of nutrient-rich water from the Estuary towards the southern GSL was clearly evident at that time of the year, while phytoplankton activity remained relatively weak in the system (based on satellite ocean colour data). Compared to 2011, the nitrate concentrations in 2012 were especially higher in the estuarine portion of the GSL (SLE, northwestern GSL) and the zone under its influence (southern GSL). Nevertheless, compared to previous observations, the winter maximum nutrient inventories in 2011, and to a lesser degree in 2012, were below the 2002–2010 average in many areas of the Estuary and GSL (Fig. 9). This pattern appears to have begun in 2008, as revealed by the increased frequency of strong negative anomalies across various subregions, with the strongest negative anomalies in 2010 (Fig. 10). The timing of the survey does not appear to be a factor.

During the late spring (June) surveys of 2011 and 2012, surface nitrate inventories were low compared to late winter inventories along the seven sections crossing the Estuary and GSL due to utilization by phytoplankton (Fig. 11). The depletion of nutrients in the surface layers was more pronounced in the eastern, southern, and central parts of the GSL compared to the Estuary and northwestern GSL, as previously observed. During the fall 2011 and 2012 surveys, surface nitrate levels were comparable or only somewhat higher than those measured during the late spring survey for most areas except for the estuarine portion of the GSL in 2012

(especially TSI and TASO; Fig. 11). This indicates that the autumnal turnover had not occurred or had just begun in many regions.

The late spring nitrate inventories in 2011 and 2012 were markedly below the 1999–2010 reference period averages for most areas of the Estuary and GSL (Fig. 10). In 2011, the differences between the winter maximum inventories and the late spring minimum inventories along the sections were also overall well below the 1999–2010 average while these differences were much more variable across the seven sections in 2012. This index represents the pool of nutrients that was potentially used by phytoplankton during spring. A negative index indicates lower new phytoplankton production rates with potential detrimental effects on higher trophic levels.

In fall, surface nitrate inventories in 2011 and 2012 were overall below the 1999–2010 average except in the SLE and northwestern GSL in 2012 (Fig. 10).This may suggest that the autumnal turnover was largely delayed compared to the 1999–2010 reference period, especially in 2012. Finally, close examination of the standardized scorecard anomalies reveals that spring and fall surface nitrate inventories (similar to winter inventories) have tended to be predominately strongly negative since 2010 (Fig. 10), probably reflecting the strong warming event during this period.

Overall, chlorophyll levels in 2011 and 2012 were relatively low during the spring and fall surveys for most areas of the GSL. The exceptions were the SLE and northwestern GSL along the Gaspé Peninsula during the spring survey, as previously observed (Fig. 10 and 12).

Remote sensing of ocean colour

Satellite ocean colour data provide large-scale images of surface phytoplankton biomass (chlorophyll *a*) over the whole NW Atlantic. We used two-week satellite composite images of GSL subregions to supplement our ship-based observations and provide seasonal coverage and a large-scale context over which to interpret our survey data. The ocean colour imagery provides information about the timing and spatial extent of the spring and fall blooms but does not provide information on the dynamics that take place below the top few metres of the water column. In addition, satellite ocean colour data for the SLE are largely contaminated by high concentrations of nonchlorophyllous matter originating from the continent (such as suspended particulates and coloured dissolved organic matter) that render these data too uncertain to be used. Knowledge of phytoplankton dynamics in the SLE and the subsurface information are gathered using the high-frequency sampling at Rimouski station and the broad-scale oceanographic surveys.

Satellite images in 2011 and 2012 revealed considerable spatial variability in the timing of the spring bloom in the GSL (Fig. 13), as has been previously observed (not shown), which may be due to subregional differences in the timing of sea-ice melt and the onset of water column stratification (Le Fouest et al. 2005). The spring phytoplankton bloom occurred between March and May, depending on the region, and started earlier in the northwest and southern parts of the GSL (Fig. 13). The MODIS imagery confirmed the initiation of the spring bloom in the southern part of the GSL at the end of the helicopter survey in 2012 (Fig. 13). A similar phenomenon was observed in 2010. This may explain the exceptionally low nitrate levels in this region at that time of the year. The MODIS imagery also confirmed the overall low surface chlorophyll levels observed during our late spring and fall surveys during 2011 and 2012 (not shown). Finally, satellite images revealed that the fall blooms in the GSL in 2011 and 2012 were much weaker in magnitude compared to spring blooms, as previously observed (Fig. 14).

Observations from six GSL subregions indicate that the magnitude of surface phytoplankton bloom detected by the MODIS satellite was generally stronger in 2012 than in 2011

(Fig. 14, 15). In addition, surface blooms occurred much earlier in many of the subregions and in some cases were longer in duration in 2012 relative to the patterns noted previously. In contrast, summer and fall chlorophyll levels were extremely weak in 2012 relative to previous years for the entire GSL. In 2011, the magnitude of surface phytoplankton bloom and the fall levels were much more variable across the six statistical subregions, being either close to, below, or above the 2003–2010 mean.

The standardized scorecard anomalies inferred from the MODIS satellite imagery showed some interesting patterns across the statistical subregions (Fig. 15). A shift to earlier timing of the spring bloom is especially evident in the increased frequency of negative anomalies since 2010 across many of the subregions. In addition, anomalies of chlorophyll levels, especially during summer and fall, have tended to be predominately negative since 2010.

ZOOPLANKTON

Fixed stations

The long-term (1999–2010; Rimouski: 2005–2010) seasonal climatologies of zooplankton biomass at the four fixed stations are shown along with observations made in 2011 and 2012 in Figure 16. The zooplankton biomass at Rimouski station in 2011 and 2012 was slightly below average in summer but above the long-term seasonal average in fall (Fig. 16a); it was also somewhat above the long-term average in April–May 2012. At Shediac station, zooplankton biomass was generally lower than normal in May–June 2011 and near normal later in the season in both 2011 and 2012, with only one observation well above the normal in June 2012 (Fig. 16d). However, these results must be considered carefully due to low sampling frequency.

The seasonal zooplankton biomass climatologies were similar for the two deep fixed stations (Rimouski and Anticosti Gyre), with minima observed in early summer and increases to fall maxima (Fig. 16 a, b). Examination of the seasonal climatology (2005–2010) in zooplankton biomass and *Calanus* species abundance in two different depth layers (0–100 m, 100–320 m) at Rimouski station confirmed that deep-dwelling (>100 m) late development stages drive the biomass signal at the deep sampling sites (Fig. 17). The seasonal climatology of zooplankton biomass at Gaspé Current and Shediac stations were also alike, with low biomass in winter and early spring, a well-defined maximum in late spring and early summer, and a much lower biomass from mid-summer into fall (Fig. 16c, d).

Total abundances and relative proportions of the 10 dominant copepod species determined from data collected at all fixed sites are shown in Figures 18 and 19. Total copepod abundance was above normal from July to September 2011 at Rimouski station but similar to the long-term average during the rest of 2011 and throughout 2012 (Fig. 18a). This period of greater-than-normal copepod abundance in 2011 was associated with a greater proportion of small copepods (small calanoids, cyclopoids) in the population; this pattern was also apparent at the other fixed sites (Fig. 18g, 19c, g). The relative proportions of the 10 dominant copepod species in 2012 were closer to normal across all sites, i.e., a higher proportion of large-bodied zooplankton of the genera *Calanus* and *Metridia* in the population. At Gaspé Current and Shediac stations, the observed total copepod abundance was highly variable among sampling events, possibly an artifact of the low sampling frequency in a region influenced by the dynamic Gaspé Current. This variability and sparse sampling precluded any confident comparison with the long-term seasonal climatology.

The abundance of *C. finmarchicus* was generally below the long-term average at the fixed sites in 2011 and 2012 (Fig. 20, 21). At Rimouski station, only a few observations were above average in late summer 2011 and early summer 2012 (Fig. 20a). The population stage structure

in 2011 differed from the long-term average, with a stronger peak in CI–III stages occurring from June to August relative to a peak generally taking place in June–July (Fig. 18b, c). In 2012, a first peak in CI–III occurred during the same period as seen in the long-term climatology in early summer but was followed by a pronounced autumn peak, suggesting the production of a second generation stronger than usually observed at this site (Fig. 20d). Despite a more sporadic seasonal coverage at the other fixed stations, the stage structure suggested that the CI–III peak might have occurred earlier (or was shorter) in 2011 and 2012 than normal (Fig. 20g, h, 21). At Gaspé Current and Shediac stations, the 2012 pattern in stage composition was similar to the long-term climatology (Fig. 21).

Abundance of the large-bodied *C. hyperboreus* was near or above the long-term average in 2011 and 2012 at Rimouski station (Fig. 22). During both years, abundance was above normal from August to October, with higher abundance in April 2012 relative to April 2011 (Fig. 22). Because of sparser sampling, it is more difficult to describe the abundance patterns at the other sites (Fig. 22, 23), although abundance appeared to be greater than normal in summer and fall at the Anticosti Gyre station in 2012. The relative CI–III copepodite abundance was mostly similar to the long-term climatology, albeit with a shorter duration of CI–III in 2011 and 2012 (until June) in comparison to the long-term average (until July) at Rimouski station (Fig. 22). At all sampling sites, the relative proportion of CIV from July to late fall in 2011 and 2012 appeared to be greater than the long-term climatology, indicating potential changes in population development and dynamics (Fig. 22, 23). Examination of the stage structure revealed that sampling in late winter and spring is critical in order to describe the recruitment period of early copepodite stages in this species, a task rarely achieved over the last few years at Anticosti Gyre and Gaspé Current stations (Fig. 2, 22, 23).

The fall increases in zooplankton biomass at the two deep fixed stations (Rimouski and Anticosti Gyre) (Fig. 16a, b) were associated with increased abundances of late development stages of *C. finmarchicus* and *C. hyperboreus* (Fig. 20, 22). At the shallow stations (Gaspé Current and Shediac), zooplankton biomass could also be related to *C. finmarchicus* and *C. hyperboreus* abundance (Fig. 21, 23). Considering the abundance patterns of *Calanus* spp. in the different layers of the water column (Fig. 17), we can conclude that zooplankton biomass at the deep sampling sites mainly reflects the zooplankton community dominated by late stages of *Calanus* species overwintering in the deeper part of the GSL while zooplankton biomass at the shallow stations is determined by the active components of the *C. finmarchicus* and *C. hyperboreus* populations (Plourde et al. 2001, 2003).

The abundance of small calanoids (*Pseudocalanus* spp.) was strikingly different between 2011 and 2012 at Rimouski station (Fig. 24). In 2011, abundance was greater than the long-term average from July onward, while it remained mostly below the normal in 2012 (Fig. 24a). The same pattern was observed to some extent at the sparsely sampled Anticosti Gyre and Gaspé Current stations (Fig. 24e, 25a). At Rimouski station, population abundance minima similar to the long-term average were observed from April to June in both years (Fig. 24a). Population stage composition averaged from 1999 to 2010 showed that early stages were observed throughout the year (potential for several generations) at Rimouski, Anticosti Gyre, and Gaspé Current stations (Fig. 24b, f, 25b) (stage composition is not available for Shediac station). However, recruitment to early stages was restricted from late spring to September at Rimouski station in 2011 and 2012; this feature was observed only in 2012 at the other sites but is based on limited sampling (Fig. 24c, d, g, h, 25c, d).

Sections

The annual averaged total zooplankton biomass values for each section during the spring and fall surveys are shown in Figure 26. For most sections, biomass was higher in 2012 than in

2011, with biomass in 2011 being roughly equivalent to 2010 (Fig. 26). This pattern also emerged when data are presented at a broader scale, corresponding to the three distinct oceanographic subregions, i.e., the western (wGSL), southern (sGSL), and eastern (eGSL) regions (Fig. 27). Total zooplankton biomass in the sGSL in spring showed greater interannual variability than in other GSL regions and was much higher than in fall for several years; this pattern was not observed in the wGSL or eGSL (Fig. 27). These marked differences in zooplankton biomass among years in the sGSL during the early part of the productive season could reflect interannual differences in the transport of large-bodied *Calanus* spp. from deeper adjacent regions in spring and early summer (Runge et al. 1999, Maps et al. 2010). High population loss due to advection and/or natural and predation mortality of *Calanus* spp. by abundant planktivorous predators would explain the much lower biomass observed in fall relative to spring during some years.

The annual abundances of key copepod species in the three regions are shown in Figures 28, 29, and 30. The annual mean abundance of *C. finmarchicus* was similar in 2011 and 2012 in the wGSL and eGSL but greater in 2012 than in 2011 in the sGSL (Fig. 28). When a longer period is considered, *C. finmarchicus* abundances in 2011 and 2012 were lower than during the period of high abundance observed in the mid-2000s. For *C. hyperboreus*, the mean 2012 abundance was greater than in 2011 across the GSL and higher than most years in the wGSL and sGSL (Fig. 29). Total abundance of this species appeared to drive the interannual pattern in zooplankton biomass, although the increase in zooplankton biomass from 2011 to 2012 appeared smaller than what would have been expected based on *Calanus* species abundance (Fig. 28, 29). The mean annual *Pseudocalanus* spp. abundance was lower in 2012 relative to 2011 in all regions, and the abundances for both years were lower than the 2010 maximum, which was the culminating point of a period of increasing abundance that started in 2005 (Fig. 30).

Copepod phenology

We present a detailed figure showing the seasonal cycle of the relative proportions of *C. finmarchicus* copepodite stages at Rimouski station from 1994 to 2012 in order to provide—for the first time—an assessment of potential changes in the phenology of zooplankton in the GSL (Fig. 31). We used proportions to minimize any distortion caused by large interannual variations in absolute abundance (see Fig. 20a, 32). The comprehensive examination of this data set revealed notable changes in the timing of the development of this key copepod species. For example, the period of maximum contribution of stages CI–III (equivalent to their abundance maximum) shifted from mid to late July during the 1994–2000 period to predominantly mid-June to early July in 2006–2012 (Fig. 31). This trend toward earlier development in summer stages was also observed in CIV and CV stages (Fig. 31). The occurrence of a second generation of CI–III and CIV in late summer and/or late fall was also more common from 2003 to 2012 than during previous years (see light blue to orange areas from August to October in Fig. 31). Long-term changes in the timing of maximum occurrence were also observed for stage CVI (both sexes), with an earlier timing from 2008–2012 relative to 1994–2005 (Fig. 31). These changes in the phenology of *C. finmarchicus* mirrored those in the stage structure of the overwintering population of *C. hyperboreus* (data not shown), suggesting that variations in the physical, chemical, and biological environmental conditions influence the intrinsic dynamics of these key copepod species, not only their overall abundance and productivity.

Scorecards

A synthesis of basic AZMP zooplankton indices (abundances of *C. finmarchicus*, *Pseudocalanus* spp., total copepods, non-copepods) was performed using annual standardized

abundance anomalies and is presented as a scorecard (Fig. 32). In general, these annual indices were relatively coherent through the time series among the fixed stations, sections, and large regions. After two years of strong negative abundance anomalies in 2009 and 2010, *C. finmarchicus* remained below normal in all regions (in the sGSL in particular) in 2011 but increased to near-normal values in 2012. The smaller *Pseudocalanus* spp. showed the opposite pattern, with a high positive abundance anomaly in 2011 in all regions following two years of abundances well above the normal in 2009–2010 and a decrease to near-normal abundance in 2012. Total copepod abundance was generally close to the long-term normal in 2011 but showed a negative anomaly in 2012. Finally, a strong positive anomaly in non-copepod abundance (by up to four standard deviations) in the eGSL was observed in 2011; it decreased markedly in 2012 to near-normal values in the wGSL and eGSL while remaining above normal in the sGSL. This index is strongly influenced by meroplankton taxa (larval stages of various benthic invertebrates) and larval euphausid stages (eggs, nauplii).

The annual standardized abundance anomalies for a new set of zooplankton indices are presented in Figure 33. Again, these annual indices were relatively coherent among the fixed stations, sections, and large regions over the time series. *C. hyperboreus* abundance was well above the long-term normal in 2012 after the near- to below-normal values in 2011; this coincided with the *C. finmarchicus* increase between 2011 and 2012 (Fig. 32) and resulted in a larger-than-normal abundance of large calanoids in 2012 (Fig. 33). This positive anomaly in large-bodied copepods has not been observed in the GSL since 2008. Overall, small calanoid abundances remained near or above normal in 2011 and 2012, indicating that the decrease in *Pseudocalanus* spp. in 2012 (Fig. 32) was compensated by an increase in the abundance of other taxa. Most notably, the warm-water species *Centropages* spp. and *Paracalanus* spp. showed their highest abundances of the time series (strong positive anomaly) in 2011 and 2012 (Fig. 33). Considering the GSL as a whole, the small cyclopoids (dominated by *Oithona* spp.) were below or near normal in 2011 and 2012, respectively, which could have contributed to the negative total copepod anomaly observed in 2012 (Fig. 32, 33). Finally, the abundance of cold/arctic copepod species (*C. glacialis*, *M. longa*) was well above normal in 2011 but showed a marked decrease to near-normal abundance in 2012 (Fig. 33).

DISCUSSION

In 2011 and 2012, a set of physical indices, including surface and cold intermediate layer temperature as well as ice season duration, indicated temperature conditions well above the normal; this trend had begun in 2010 (Galbraith et al. 2013). In 2012, this composite index showed its highest value since 1980 and the second highest since 1971; additionally, deep-water temperature in the GSL sharply increased in 2012 to values seldom observed since the early 1980s (Galbraith et al. 2013). Therefore, the present document reports on chemical and biological conditions in the GSL in the context of a strong warming event that began in 2008, which was the last year with a below-average surface temperature index in the GSL (Galbraith et al. 2013).

Winter maximum nutrient inventories in 2011, and to a lesser degree in 2012, were below the 2002–2010 average in many areas of the Estuary and GSL. This trend has been evident since 2008, as revealed by the increased frequency of strong negative anomalies across various GSL subregions. Winter mixing is a critical process to bring nutrient-rich deep water to the surface. In the GSL, this winter convection is in part caused by buoyancy loss (cooling and reduced runoff), brine rejection associated with sea-ice formation, and wind-driven mixing prior to ice formation (Galbraith 2006). In 2011 and 2012, the higher-than-normal average water temperature/stratification and the lower-than-normal ice formation (Galbraith et al. 2013) may have reduced the thickness of the vertical mixing, which limited the supply of start-up nutrients

for primary producers (Plourde and Therriault 2004) and therefore reduced total annual primary production. In addition to vertical mixing, a reduction in upwelling at the head of Laurentian Channel and/or of transport of nutrients via the Gaspé Current may also have contributed to the below-normal winter nutrient inventories for the estuarine portion and freshwater-influenced subregions of the GSL, notably in 2011. In contrast to expectations, the remote sensing of ocean colour data nevertheless revealed that the magnitude of the spring phytoplankton blooms in many areas of the GSL was above normal, especially in 2012.

Changes in stratification can have either positive or negative effects on primary production depending on water column conditions (Ferland et al. 2011). Changes in the ice cover can also influence primary production by its influence on the light conditions in the water column (Le Fouest et al. 2005). The low ice volume and the higher-than-normal average stratification (Galbraith et al. 2013) may have contributed to the markedly early but sometimes intense spring blooms in recent years. On the other hand, the persistence of strong stratification during spring, summer, and fall in 2011 and especially in 2012 (Galbraith et al. 2013) may have reduced phytoplankton production by inhibiting nutrient mixing into surface waters, as is suggested by the strong prevalence of below-normal chlorophyll and nitrate levels observed since 2010 during the post spring-bloom period.

In the lower St. Lawrence Estuary, the situation is somewhat different: the timing of the bloom was relatively close to the normal in 2011 and 2012. In this region, the spring bloom timing is recognized to be largely influenced by both runoff intensity and freshwater-associated turbidity (Levasseur et al. 1984, Therriault and Levasseur 1985; Zakardjian et al. 2000, Le Fouest et al. 2010, Mei et al. 2010). The spring bloom typically starts just after the spring-summer runoff peak. The shorter residence times and weak light conditions during higher freshwater runoff periods are two possible explanations for the delay in phytoplankton growth in this region in early summer compared to early spring in the GSL.

A shift to a smaller-sized phytoplankton community has also been observed in recent years at the Rimouski (since 2004) and Shediac Valley (since 2009) fixed stations, although this phenomenon was less notable in 2011–2012, especially in the St. Lawrence Estuary. In addition, the relative abundance of dinoflagellates has tended to be predominantly higher than normal in recent years. Flagellates and dinoflagellates are typical of a community dominated by recycled production than new production; this situation is consistent with higher nutrient limitation in the post-bloom period (Ferland et al. 2011). Warmer temperatures are also associated with a shift toward greater flagellate and dinoflagellate predominance (Levasseur et al. 1984, Li and Harrison 2008), with potential consequences on copepod recruitment and zooplankton composition as well as on the flow of energy in marine food webs.

In 2012, zooplankton biomass increased relative to 2011 but much less than expected from the observed increase to near normal (*C. finmarchicus*) and record high (*C. hyperboreus*) abundances of *Calanus* species (Fig.16, 32, 33). The smaller body size of *C. finmarchicus* and changes in the relative stage proportion toward a dominance of CIV (smaller than CV and CVI) in *C. hyperboreus* (Fig. 22) would explain why the increase in zooplankton biomass from 2011 and 2012 was of smaller amplitude than the increase in *Calanus* species abundance (see below).

Finding abundances of these arctic and subarctic large-bodied species to be near or well above normal during the near-record high surface temperature in 2012 appears counterintuitive. However, the active growth phase of *C. hyperboreus* occurs from April to June in the GSL, and this species migrates to its deep diapause habitat (>200 m) in early July (Fig. 17c) (Plourde et al. 2003). *C. finmarchicus* mainly reproduces and grows in spring and early summer, and enters diapause in late July to early August in the wGSL (Fig. 17b) (Plourde et al. 2001, Johnson et al.

2008). *C. finmarchicus* has also been observed to actively avoid warm and stratified surface waters in order to exploit subsurface habitats (refuges) where it can reproduce and develop (Williams 1985, Jónasdóttir and Koski 2011). In 2012, for example, temperatures > 12–13^{o}C, which are potentially detrimental for the physiology of *C. finmarchicus* late stages, were restricted to the upper 20 m, a depth below which subsurface phytoplankton blooms are commonly observed in the region (Helaouët and Beaugrand 2007, Møller et al. 2012, Galbraith et al. 2013). These characteristics suggest that these species may avoid or adapt their life cycle strategy to minimize the potential negative impacts of warm conditions like those observed in late summer and fall 2012. However, the long-term effect of such warm conditions on the overall success of these species has yet to be determined.

Even though the overall success (abundance) of *Calanus* species was normal or above normal in 2012 despite record-high water temperatures, the warm surface conditions affected various aspects of their population dynamics (ontogeny). The greater relative proportion of CIV in overwintering *C. hyperboreus* in fall 2011 and 2012 relative to the long-term climatology suggests a change in the development rate and the overall life cycle strategy of this species (Plourde et al. 2003). Changes toward an earlier period of high CVI abundance and recruitment to early stages CI–III as well as evidence for a more predominant second generation in fall were also observed in *C. finmarchicus* over the last decade (Fig. 31). Moreover, *C. finmarchicus* CV in fall 2012 were smaller than usual in the GSL while the body size of CVIf captured at Rimouski station has shown a long-term negative trend since the cold period in the mid-1990s (Plourde et al. 2013). These modifications to the phenology are evidence of the direct effects of changes in the physical (ice dynamics, surface temperature) and biological (phytoplankton bloom timing, duration, and amplitude) environment that have occurred in the region over the last few years (Plourde et al. 2013). In the long term, changes in the body size of *Calanus* species could affect the fecundity potential and overwintering capacity of CVIf, which are likely mediated by energy storage (Plourde et al. 2001, 2003, Maps et al. 2010). Overall, changes in phenology and body size detected in *Calanus* species were relatively strong; these could be useful indices to implement in AZMP to measure the effects of climate change on the dynamics of lower trophic levels in the ecosystem.

The small calanoids showed marked changes in 2011 and 2012 relative to previous years that could be associated with concomitant changes in environmental conditions (Fig. 32, 33). Most of these small species appear to thrive in summer and fall following the peak in surface-dwelling *Calanus* species abundance in spring and early summer, suggesting that abnormally high water temperatures in late summer and fall 2012 (and in 2011 to a lesser extent) might have influenced their success in the region (Plourde et al. 2002). The abundance of *Pseudocalanus* spp., a species complex observed from Georges Bank to the Canadian Arctic and widely distributed in the GSL, decreased to near normal from 2011 to 2012, while warm-water species such as *Paracalanus* spp. and *Centropages* spp. (*C. typicus* in particular) showed record-high abundances in 2011 and 2012. High abundances of warm-water species (> 6 standard deviations above normal) were observed in the shallow sGSL and the eGSL in 2012 (Fig. 33); both of these regions were much warmer than the wGSL in summer and fall and were directly affected by water originating from the adjacent continental shelf (Galbraith et al. 2013). The increased abundance of warm-water species in 2011 and 2012 was associated with the marked warming of the GSL initiated in 2010 (Galbraith et al. 2013).

The abundances of cold/arctic species (*C. glacialis*, *M. longa*) were well above normal in 2011 and remained near normal in the very warm conditions observed in 2012. Intuitively, one would have expected a lower abundance of cold/arctic species during these warm years, which were characterized by a strong positive anomaly in warm-water species. This apparent discrepancy could be attributed to the fact that AZMP hydrographic sections often cross distinct waters

masses of different origins. For example, the proportion of *M. longa* / (*M. longa* + *M. lucens)* and *C. glacialis* / (*C. finmarchicus* + *C. glacialis)* were greater on the northwest half (Québec side) than on the southeast half (Newfoundland side) of the TBB section in fall 2012 (not shown). While the Newfoundland end of TBB is under the influence of water entering the eGSL through Cabot Strait, waters along the northern Québec coast principally originate from the inner Labrador Shelf (Galbraith et al. 2013). A greater ratio of cold/arctic species in this area could result either from their transport through the Strait of Belle Isle from the inner Labrador Shelf, from colder local environmental conditions more suitable for these cold/arctic species, or both. Greater abundances of warm-water species such as *Centropages*, *Paracalanus,* and—for the first time—*Clausocalanus* were also observed along the Newfoundland coast in fall 2012 on the TBB and TDC sections. These observations reinforce the transitional status of the GSL, which is located between the colder "upstream" Labrador/Newfoundland shelf and the more temperate "downstream" Scotian Shelf. Finally, identification of the morphologically similar species *C. finmarchicus* / *C. glacialis* (and potentially *M. lucens* / M. *longa*) using constant body size criteria could be problematic under the varying environmental conditions prevailing at the scale of the AZMP, with a larger impact being on the rarer species (*C. glacialis* in the case of the GSL) (Parent et al. 2011, Gabrielsen et al. 2012). Therefore, these results should be considered with care until the problem is better quantified.

SUMMARY

- This document reports on the chemical and biological (plankton) conditions in the GSL in 2011 and 2012 in the context of a strong warming event initiated in 2008. Data from these two years are compared to time-series observations starting in 1999.
- One of the most prominent events in 2011–2012 is that winter, spring, and fall surface nitrate inventories were below normal in many regions of the Gulf, probably due to the persistent higher-than-normal average water temperature/stratification and the below-normal ice conditions.
- A shift to earlier timing of the spring bloom is clearly evident in the increased frequency of strong negative anomalies since 2010 across all subregions of the GSL. In addition, chlorophyll levels during summer and fall have tended to be below normal since 2010.
- There is evidence of a shift to a smaller phytoplankton community and higher relative abundance of dinoflagellates at the Rimouski and Shediac Valley stations that began in 2004.
- The seasonal zooplankton biomass climatologies were similar at the two deep fixed stations (Rimouski, Anticosti Gyre) and showed fall maxima associated with increased abundances of *Calanus* spp., especially in the deep water layer. Biomass climatologies were also similar at the shallow stations (Gaspé Current, Shediac), again largely due to surface-dwelling *Calanus* spp. abundances. Biomass in 2012 increased relative to 2011.
- In 2011 and 2012, fixed station abundances of *C. finmarchicus* were below and those of *C. hyperboreus* near or above the 1999–2010 long-term averages. The abundance of small calanoids (*Pseudocalanus* spp.) was strikingly different between 2011 and 2012 at Rimouski station: greater in late 2011 while normal or below normal in 2012.
- There is evidence of ontogenetic and phenological changes in *Calanus* species that appear to be the direct effects of the warmer environmental conditions experienced by the region over the last few years. Variations in the physical, chemical, and biological environmental conditions influence the intrinsic dynamics of these key copepod species,

not only their overall abundance and productivity. These changes could prove to be useful indices to measure the effects of climate change on lower trophic levels of the ecosystem.

- Total zooplankton biomass was higher in 2012 than in 2011, but lower than expected based on *Calanus* species abundances alone, likely because the stage CIV proportion (relative to older/larger stages) of the large-bodied *C. hyperboreus* was higher than usual.
- Total zooplankton biomass in the sGSL in spring showed greater interannual variability than in other GSL regions and was much higher than in fall for several years. This pattern was not observed in the wGSL or eGSL, which may be due to advection and/or mortality (natural or predation).
- All standard zooplankton abundance indices were relatively coherent through the time series among fixed stations, sections, and large subregions. *C. finmarchicus* and total copepod abundances were at or somewhat below normal in 2011–2012 while *Pseudocalanus* spp. and non-copepod abundance indices were strongly positive.
- High abundances of arctic and subarctic large-bodied species occurred simultaneously with the near-record high surface temperature in 2012, suggesting that these species avoid or adapt their life cycle strategy to minimize potential negative effects of warm conditions; the long-term effects of such high temperatures remain unknown.
- There was an increased abundance of warm-water species (*Paracalanus* spp. and *Centropages* spp.) in 2011–2012 associated with marked warming that started in 2010.
- High abundances of cold/arctic species concomitant with those of warm-water species likely reflect the complex hydrography of the GSL system and point out its position as a transitional zone between the “upstream” Labrador/Newfoundland shelf and the “downstream” Scotian Shelf.

ACKNOWLEDGEMENTS

We thank Jean-Yves Couture and Sylvie Lessard as well as Isabelle St-Pierre and Caroline Lafleur for preparation and standardization of the phytoplankton and zooplankton data, respectively. The data used in this report would not be available without the work of François Villeneuve and his team (Sylvain Chartrand, Rémi Desmarais, Marie-Lynn Dubé, Yves Gagnon, Line McLaughlin, Roger Pigeon, Daniel Thibault, and the late Sylvain Cantin) for organizing and carrying out AZMP cruises. Marie-France Beaulieu performed all zooplankton sample analyses. We thank Jeff Spry for providing data from the Shediac Valley fixed station and BIO’s remote sensing unit for the composite satellite images.

REFERENCES

Brickman, D., and B. Petrie. 2003. Nitrate, silicate and phosphate atlas for the Gulf of St. Lawrence. Can. Tech. Rep. Hydrogr Ocean Sci. 231: xi+152 pp.

DFO. 2013. Oceanographic conditions in the Atlantic zone in 2012. DFO Can. Sci. Advis. Sec. Sci. Advis. Rep. 2013/057.

Ferland, J., M. Gosselin, and M. Starr. 2011. Environmental control of summer primary production in the Hudson Bay system: The role of stratification. J. Mar. Syst. 88(3): 385–400.

Gabrielsen, T. M., B. Merkel, J. E. Soreide, E. Johansson-Karlsson, A. Bailey, D. Vogedes, H. Nygard, O. Varpe, and J. Berge. 2012. Potential misidentifications of two climate indicator species of the marine arctic ecosystem: *Calanus glacialis* and *C. finmarchicus*. Polar Biol. 35(11): 1621–1628.

Galbraith, P. S. 2006. Winter water masses in the Gulf of St. Lawrence. J. Geophys. Res., 111, C06022, doi:10.1029/2005JC003159.

Galbraith, P. S., R. Desmarais, R. Pigeon, and S. Cantin. 2006. Ten years of monitoring winter water masses in the Gulf of St. Lawrence by helicopter. AZMP Bulletin PMZA 5: 32–35 (http://www.meds-sdmm.dfo-mpo.gc.ca/isdm-gdsi/azmp-pmza/docs/bulletin_5_08.pdf).

Galbraith, P. S., J. Chassé, D. Gilbert, P. Larouche, D. Brickman, B. Pettigrew, L. Devine, A. Gosselin, R. G. Pettipas, and C. Lafleur, 2012. Physical oceanographic conditions in the Gulf of St. Lawrence in 2011. DFO Can. Sci. Advis. Sec. Res. Doc. 2012/023. iii + 85 pp.

Galbraith, P. S., J. Chassé, P. Larouche, D. Gilbert, D. Brickman, B. Pettigrew, L. Devine, and C. Lafleur. 2013. Physical oceanographic conditions in the Gulf of St. Lawrence in 2012. DFO Can. Sci. Advis. Sec. Res. Doc. 2013/026: v + 90 pp.

Helaouët, P., and G. Beaugrand. 2007. Macroecology of *Calanus finmarchicus* and *C. helgolandicus* in the North Atlantic Ocean and adjacent seas. Mar. Ecol. Prog. Ser. 345: 147–165.

Johnson, C. L., A. W. Leising, J. A. Runge, E. J. H. Head, P. Pepin, S. Plourde, and E. G. Durbin. 2008. Characteristics of *Calanus finmarchicus* dormancy patterns in the Northwest Atlantic. ICES J. Mar. Sci. 65(3): 339–350.

Jónasdóttir, S. H., and M. Koski. 2011. Biological processes in the North Sea: comparison of *Calanus helgolandicus* and *Calanus finmarchicus* vertical distribution and production. J. Plankton Res. 33: 85–103.

Koutitonsky, V. G., and G. L. Bugden. 1991. The physical oceanography of the Gulf of St. Lawrence: a review with emphasis on the synoptic variability of the motion. In: J.-C. Therriault (ed.) The Gulf of St. Lawrence: small ocean or big estuary? Can. Spec. Publ. Fish. Aquat. Sci. 113: 57–90.

Le Fouest, V., B. Zakardjian, F. Saucier, and M. Starr. 2005. Seasonal versus synoptic variability in planktonic production in a high-latitude marginal sea: the Gulf of St. Lawrence (Canada). J. Geophys. Res. 110, C09012, doi 10.1029/2004JC002423.

Le Fouest, V., B. Zakardjian, and F. J. Saucier. 2010. Plankton ecosystem response to freshwater-associated bulk turbidity in the subarctic Gulf of St. Lawrence (Canada): A modelling study. J. Mar. Syst. 81(1–2): 75–85.

Levasseur, M., J.-C. Therriault, and L. Legendre 1984. Hierarchical control of phytoplankton succession by physical factors. Mar. Ecol. Prog. Ser. 19: 211–222.

Li, W. K. W., and W. G. Harrison. 2008. Propagation of an atmospheric climate signal to phytoplankton in a small marine basin. Limnol. Oceanogr. 53(5): 1734–1745.

Maps, F., S. Plourde, and B. Zakardjian. 2010. The control of dormancy by lipid metabolism in *Calanus finmarchicus*: a population model test. Mar. Ecol. Prog. Ser. 403:165–180.

Møller, E. F., M. Maar, S. H. Jónasdóttir, T. G. Nielsen, and K. Tönnesson. 2012. The effect of changes in temperature and food on the development of *Calanus finmarchicus* and *Calanus helgolandicus* populations. Limnol. Oceanogr. 57: 211–220.

Mei, Z. P., F. Saucier, V. Le Fouest, B. Zakardjian, S. Sennville, H. Huixiang Xie, and M. Starr. 2010. Modeling the timing of spring phytoplankton bloom and biological production of the Gulf of St. Lawrence (Canada): Effects of colored dissolved organic matter and temperature. Cont. Shelf Res. 30: 2027–2042.

Mitchell, M. R., G. Harrison, K. Pauley, A. Gagné, G. Maillet, and P. Strain. 2002. Atlantic Zonal Monitoring Program sampling protocol. Can. Tech. Rep. Hydrogr. Ocean Sci. 223, iv + 23 pp.

Parent, G., S. Plourde, and J. Turgeon. 2011. Overlapping size ranges of *Calanus* spp. off the Canadian Arctic and Atlantic Coasts: impact on species' abundances. J. Plankton Res. 33: 1654–1665, doi:10.1093/plankt/fbr072.

Perrin, G., S. Plourde, C. DiBacco, G. Winkler, and P. Sirois. 2014. Tracing the origins of *Calanus* sp. in the Saguenay-St. Lawrence Marine Park (Québec, Canada) using $\delta^{13}C$ as a marker. Mar. Ecol. Prog. Ser., 499: 89–102, doi: 10.3354/meps10651.

Plourde, J., and J.-C. Therriault. 2004. Climate variability and vertical advection of nitrates in the Gulf of St. Lawrence, Canada. Mar. Ecol. Prog. Ser., 279: 33–43.

Plourde, S., P. Joly, J. A. Runge, B. Zakardjian, and J. J. Dodson. 2001. Life cycle of *Calanus finmarchicus* in the lower St. Lawrence Estuary: imprint of circulation and late phytoplankton bloom. Can. J. Fish. Aquat. Sci. 58: 647–658.

Plourde, S., J. J. Dodson, J. A. Runge, and J.-C. Therriault. 2002. Spatial and temporal variations in copepod community structure in the lower St. Lawrence Estuary, Canada. Mar. Ecol. Prog. Ser. 230: 221–224.

Plourde, S., P. Joly, J. A. Runge, J. Dodson, and B. Zakardjian. 2003. Life cycle of *Calanus hyperboreus* in the lower St. Lawrence Estuary: is it coupled to local environmental conditions? Mar. Ecol. Prog. Ser. 255: 219–233.

Plourde, S., F. Maps, and P. Joly. 2009. Mortality and survival in early stages control recruitment in *Calanus finmarchicus*. J. Plankton Res. 31(4): 371–388.

Plourde, S., P. Galbraith, V. Lesage, F. Grégoire, H. Bourdage, J.-F. Gosselin, I. McQuinn, and M. Scarratt. 2013. Ecosystem perspective on changes and anomalies in the Gulf of St. Lawrence: a context in support of the management of the St. Lawrence beluga whale population. DFO Can. Sci. Advis. Sec. Res. Doc. 2013/129. v + 30 pp.

Runge, J. A., M. Castonguay, Y. de Lafontaine, M. Ringuette, and J. L. Beaulieu. 1999. Covariation in climate, zooplankton biomass and mackerel recruitment in the southern Gulf of St Lawrence. Fish. Oceanogr., 8: 139–149.

Therriault, J.-C., and M. Levasseur. 1985. Control of phytoplankton production in the Lower St. Lawrence Estuary: light and freshwater runoff. Nat. Can.112: 77–96.

Therriault, J.-C., B. Petrie, P. Pépin, J. Gagnon, D. Gregory, J. Helbig, A. Herman, D. Lefaivre, M. Mitchell, B. Pelchat, J. Runge, and D. Sameoto. 1998. Proposal for a Northwest Atlantic zonal monitoring program. Can. Tech. Rep. Hydrogr. Ocean Sci., 194: vii + 57 pp.

Williams, R. 1985. Vertical distribution of *Calanus finmarchicus* and *C. helgolandicus* in relation to the development of the seasonal thermocline in the Celtic Sea. Mar. Biol. 86: 145–149.

Zakardjian, B. A., Y. Gratton, and A. F. Vézina. 2000. Late spring phytoplankton bloom in the Lower St. Lawrence Estuary: the flushing hypothesis revisited. Mar. Ecol. Prog. Ser. 192: 31–48.

Table 1. List of AZMP cruises with locations, dates, and sampling activities for 2011 and 2012. The section names start with "T" (transect) followed by the French abbreviations for the geographical locations: TESL: St. Lawrence Estuary; TSI: Sept-Îles; TASO: southwest Anticosti; TIDM: Îles-de-la-Madeleine; TDC: Cabot Strait; TCEN: Gulf centre; TBB: Bonne Bay; wGSL, eGSL, and sGSL denote the western, eastern, and southern subregions of the Gulf of St. Lawrence. See Figure 1 for the map showing station locations.

Sampling			2011				2012			
group	Name	Location	Dates	Vessel	Hydro	Net	Dates	Vessel	Hydro	Net
Fixed	Rimouski	48°40.0'N/068°35.0'W	13 APR-12 OCT	Beluga I and II	19	19	03 APR-27 NOV	Beluga II	26	26
	Gaspé Current	49°14.5'N/066°12.0'W	07 FEB-23 AUG	Multiple	3	3	20 JUN-30 AUG	Multiple	3	3
	Anticosti Gyre	49°43.0'N/066°15.0'W	07 FEB-27 AUG	Multiple	4	4	29 FEB-20 AUG	Multiple	4	4
	Shediac Valley	47°47.0'N/064°02.0'W	26 MAY-29 NOV	Multiple	7	7	20 APR-02 NOV	Multiple	8	8
Total					33	33			41	41
Sections	TESL	wGSL	01-11 JUN	Teleost	7	7	02-11 JUN	Teleost	7	7
Spring	TSI	wGSL	01-11 JUN	Teleost	6	6	02-11 JUN	Teleost	6	6
	TASO	wGSL	01-11 JUN	Teleost	5	5	02-11 JUN	Teleost	5	4
	TIDM	sGSL	01-11 JUN	Teleost	10	10	02-11 JUN	Teleost	10	10
	TDC	eGSL	01-11 JUN	Teleost	6	6	02-11 JUN	Teleost	6	6
	TCEN	eGSL	01-11 JUN	Teleost	5	4	02-11 JUN	Teleost	5	5
	TBB	eGSL	01-11 JUN	Teleost	7	7	02-11 JUN	Teleost	7	7
Total					46	45			46	45
Sections	TESL	wGSL	01-14 NOV	Hudson	7	7	01-14 NOV	Hudson	7	7
Fall	TSI	wGSL	01-14 NOV	Hudson	6	6	01-14 NOV	Hudson	6	6
	TASO	wGSL	01-14 NOV	Hudson	5	5	01-14 NOV	Hudson	5	5
	TIDM	sGSL	01-14 NOV	Hudson	10	10	01-14 NOV	Hudson	10	10
	TDC	eGSL	01-14 NOV	Hudson	6	6	01-14 NOV	Hudson	6	6
	TCEN	eGSL	01-14 NOV	Hudson	5	5	01-14 NOV	Hudson	5	5
	TBB	eGSL	01-14 NOV	Hudson	7	7	01-14 NOV	Hudson	7	7
Total					46	46			46	46

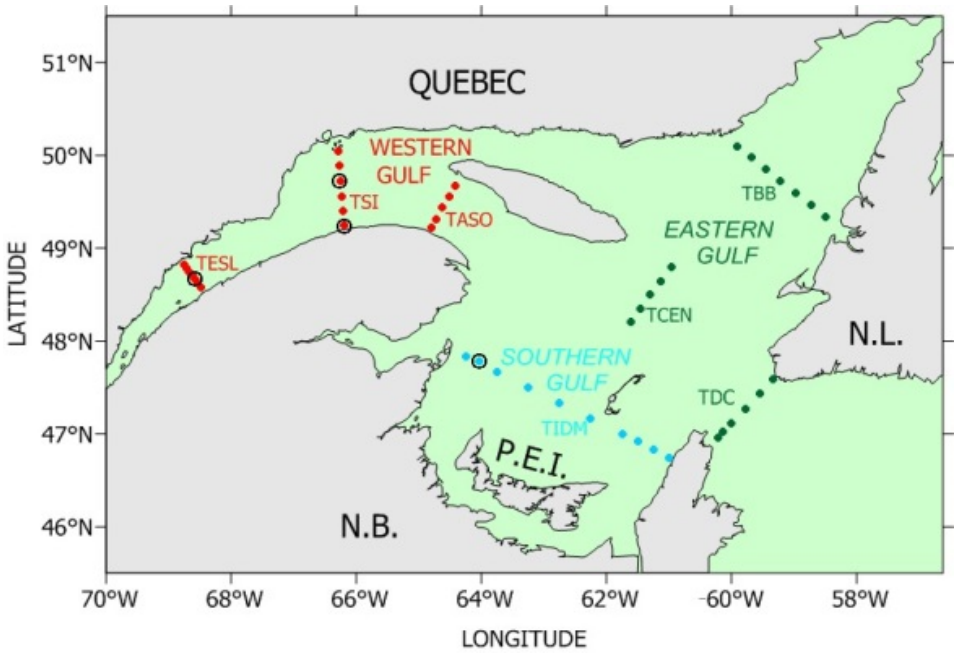

Figure 1. Map of the Estuary and Gulf of St. Lawrence showing sampling stations on the different sections (filled circles) and at fixed sites (open circles).GSL subregions are the western (red), southern (blue), and eastern (green) Gulf. The section names start with "T" (transect) followed by the French abbreviations for the geographical locations: TESL: St. Lawrence Estuary; TSI: Sept-Îles; TASO: southwest Anticosti; TIDM: Îles-de-la-Madeleine; TDC: Cabot Strait; TCEN: Gulf centre; TBB: Bonne Bay.

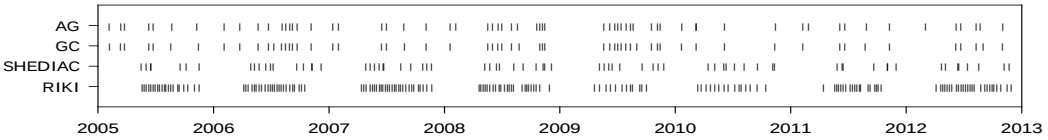

Figure 2. Sampling frequencies at the fixed stations from 2005 to 2012 to show sampling effort in recent years. AG: Anticosti Gyre; GC: Gaspé Current; RIKI: Rimouski.

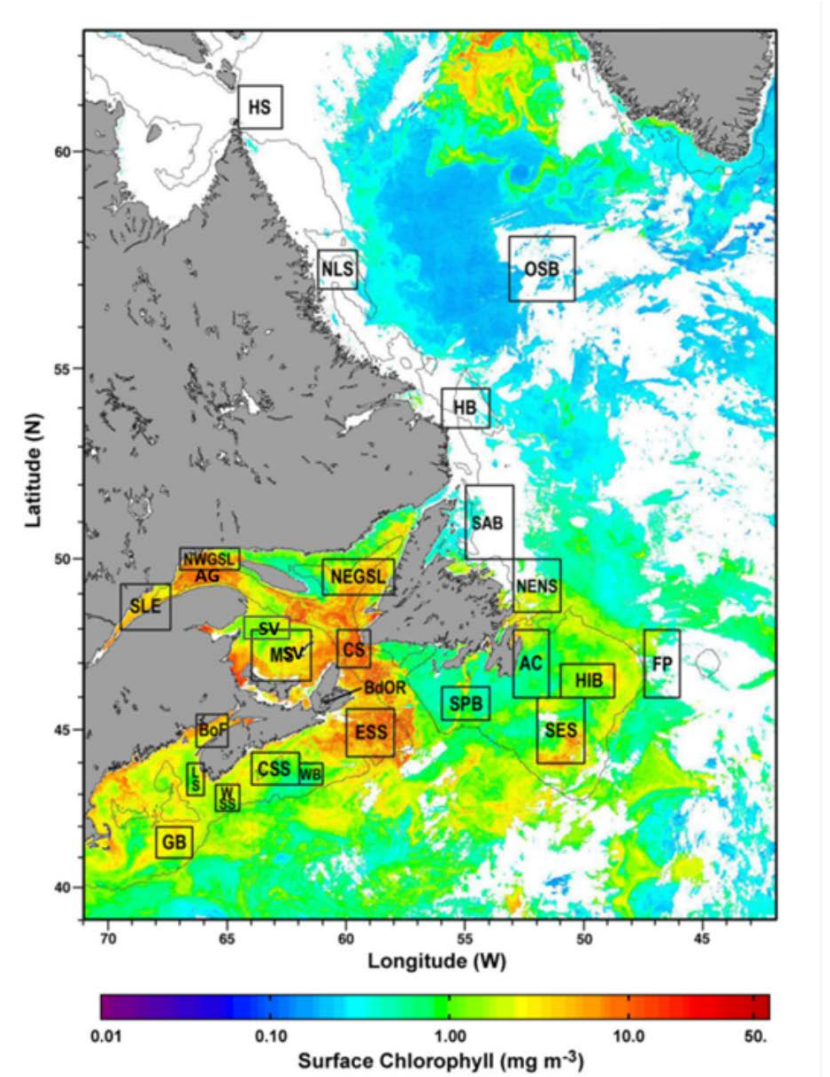

*Figure 3. Statistical subregions in the Northwest Atlantic identified for spatial/temporal analysis of satellite ocean colour data. AC: Avalon Channel; **AG**: **Anticosti Gyre**; BdOR: Bras d'Or; BoF: Bay of Fundy; **CS**: **Cabot Strait**; CSS: Central Scotian Shelf; ESS: Eastern Scotian Shelf; FP: Flemish Pass; GB: Georges Bank; HB: Hamilton Bank; HIB-Hibernia; HS: Hudson Strait; LS: Lurcher Shoal; **MS**: **Magdalen Shallows**; **NEGSL**: **Northeast Gulf of St. Lawrence**; NENS: Northeast Newfoundland Shelf; NLS: Northern Labrador Shelf; **NWGSL**: **Northwest Gulf of St. Lawrence**; OSB: Ocean Station Bravo; SAB: St. Anthony Basin; SES: Southeast Shoal; SLE: St. Lawrence Estuary; SPB: St. Pierre Bank; **SV**: **Shediac Valley**; WB: Western Bank; WSS: Western Scotian Shelf. Only data from Gulf of St. Lawrence subregions (indicated in bold) are presented in this report. (The figure is a SeaWiFS composite image showing chlorophyll a from 1–15 April 1998.)*

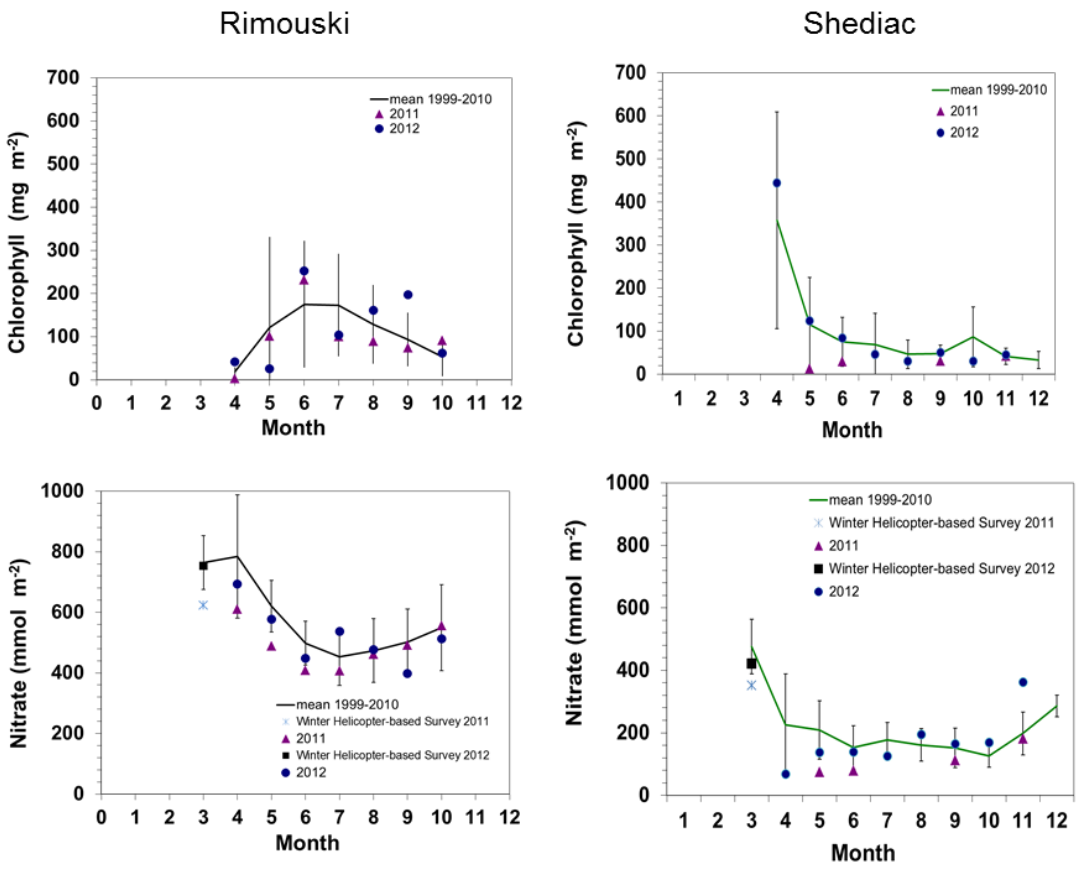

Figure 4. Comparison of 2011 (triangles) and 2012 (circles) chlorophyll (top panels) and nitrate (bottom panels) inventories with mean conditions from 1999–2010 (solid line) at the Rimouski and Shediac Valley fixed stations. Vertical lines are 95% confidence intervals of the monthly mean.Early winter nitrate values are from the March helicopter survey (samples from 2 m). Integrated values were calculated using the 2 m value × 50 m (assuming that the nitrate concentrations are homogeneous in the winter mixed layer at that time of the year).

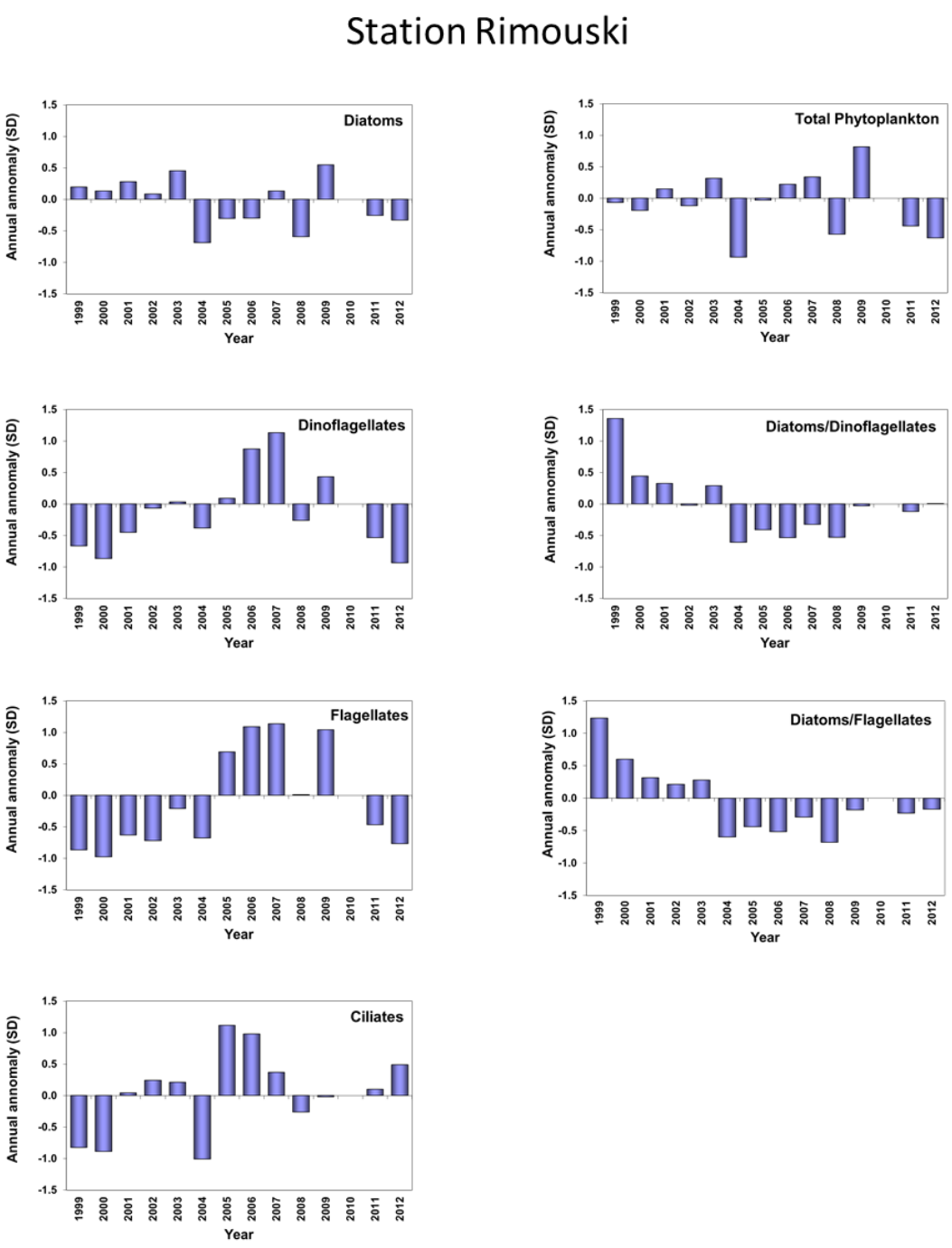

Figure 5. Time series of microplankton abundance anomalies for total phytoplankton and by group (diatoms, dinoflagellates, flagellates, ciliates), and for the diatom/dinoflagellate and diatom/dinoflagellate ratios at Rimouski station, 1999–2012.

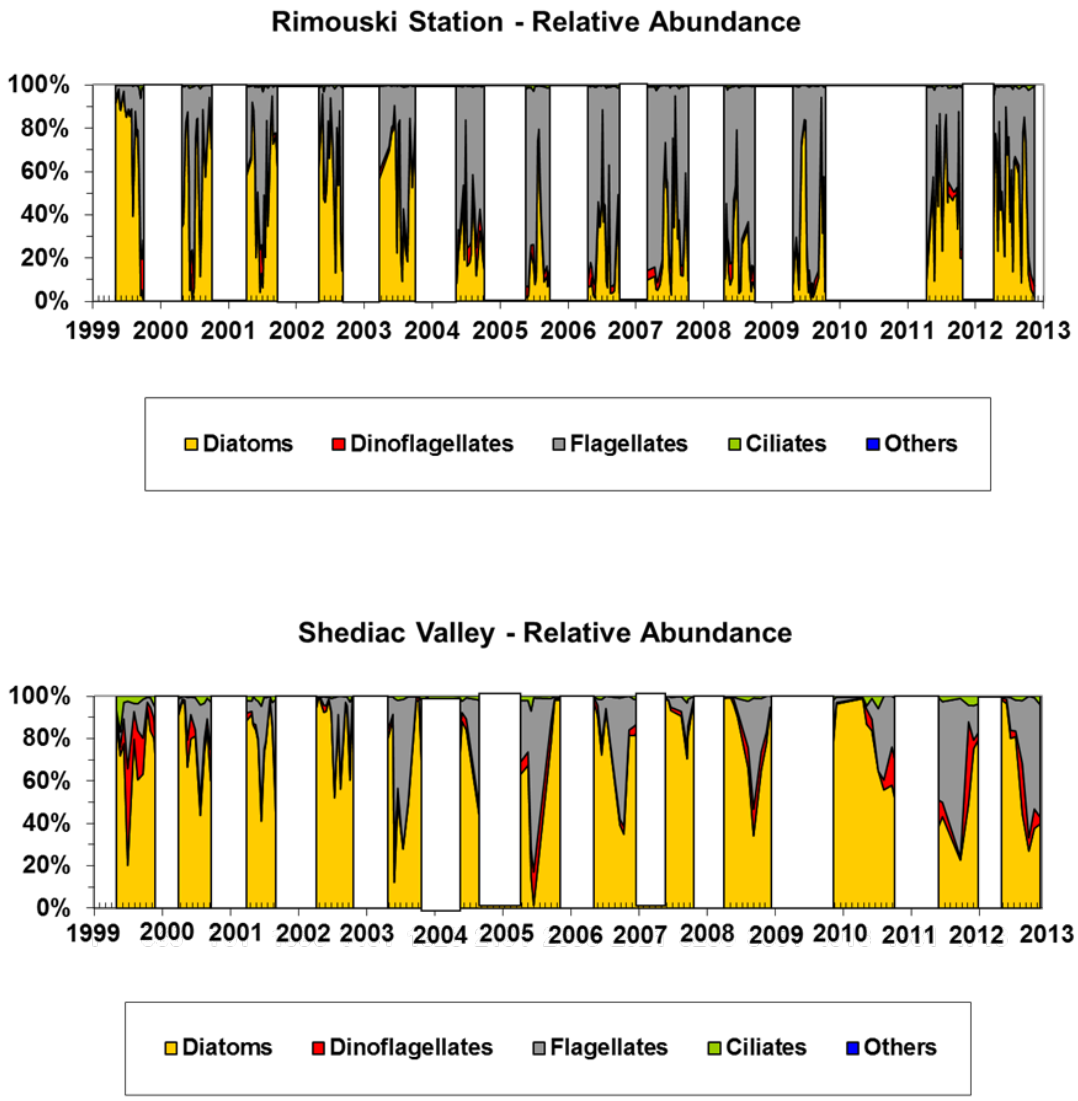

Figure 6. Phytoplankton community composition at Rimouski and Shediac Valley fixed stations, 1999–2012.

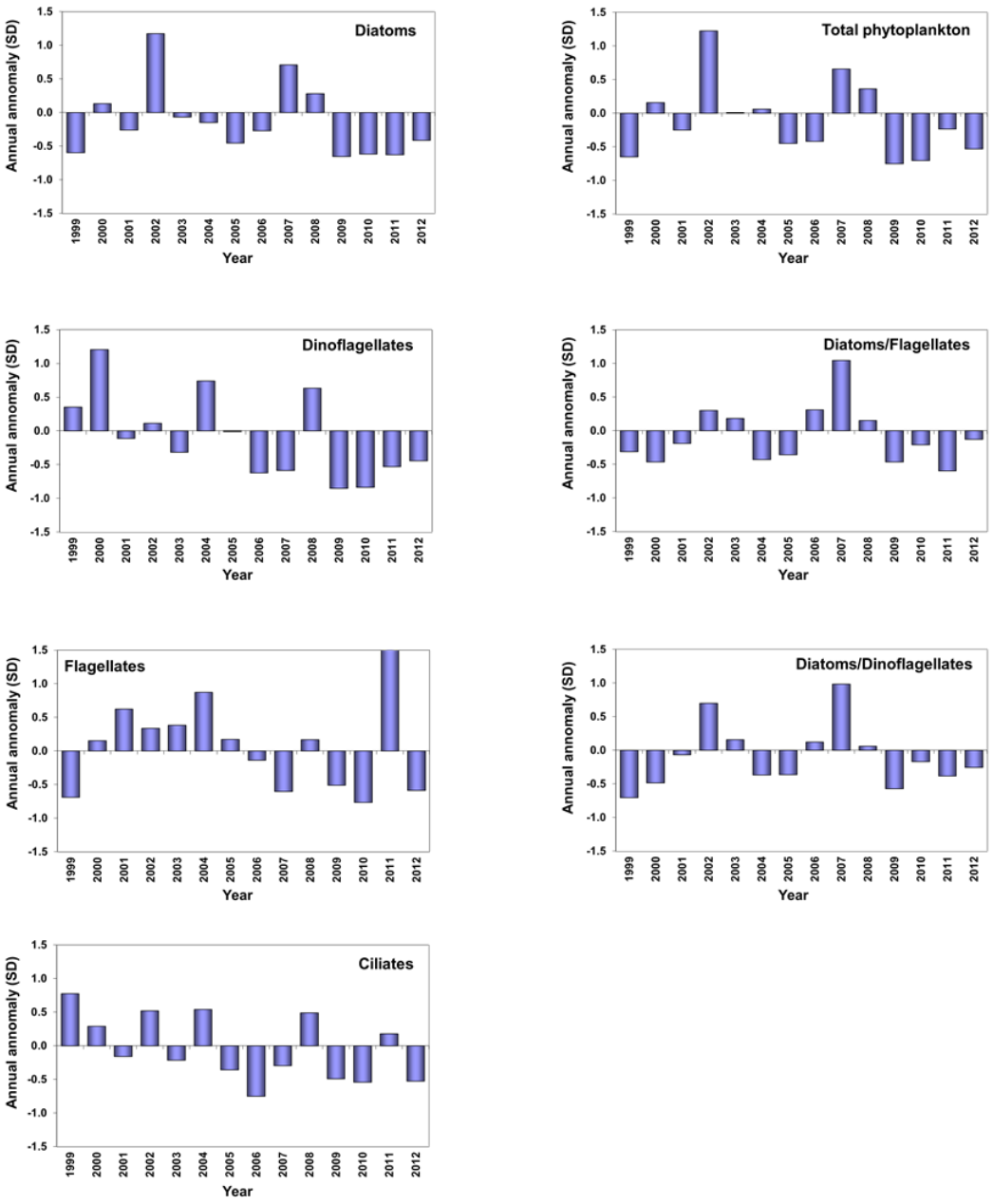

Figure 7. Time series of microplankton abundance anomalies for total phytoplankton and by group (diatoms, dinoflagellates, flagellates, ciliates), and for the diatom/dinoflagellate and diatom/dinoflagellate ratios at Shediac Valley station, 1999–2012.

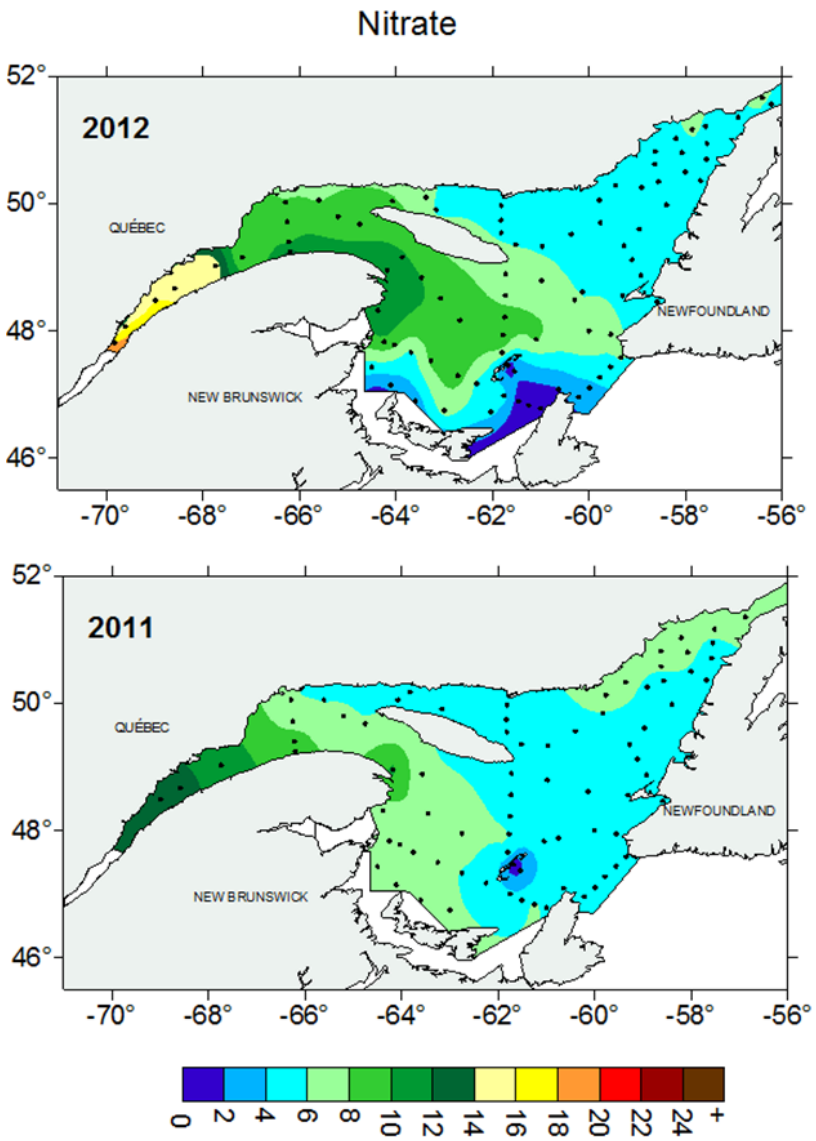

Figure 8. Concentrations of nitrate (mmol m^{-3}) at 2 m collected in the Estuary and Gulf of St. Lawrence during the helicopter survey in late winter (mid-March) 2011 and 2012. Dots indicate sampling locations.

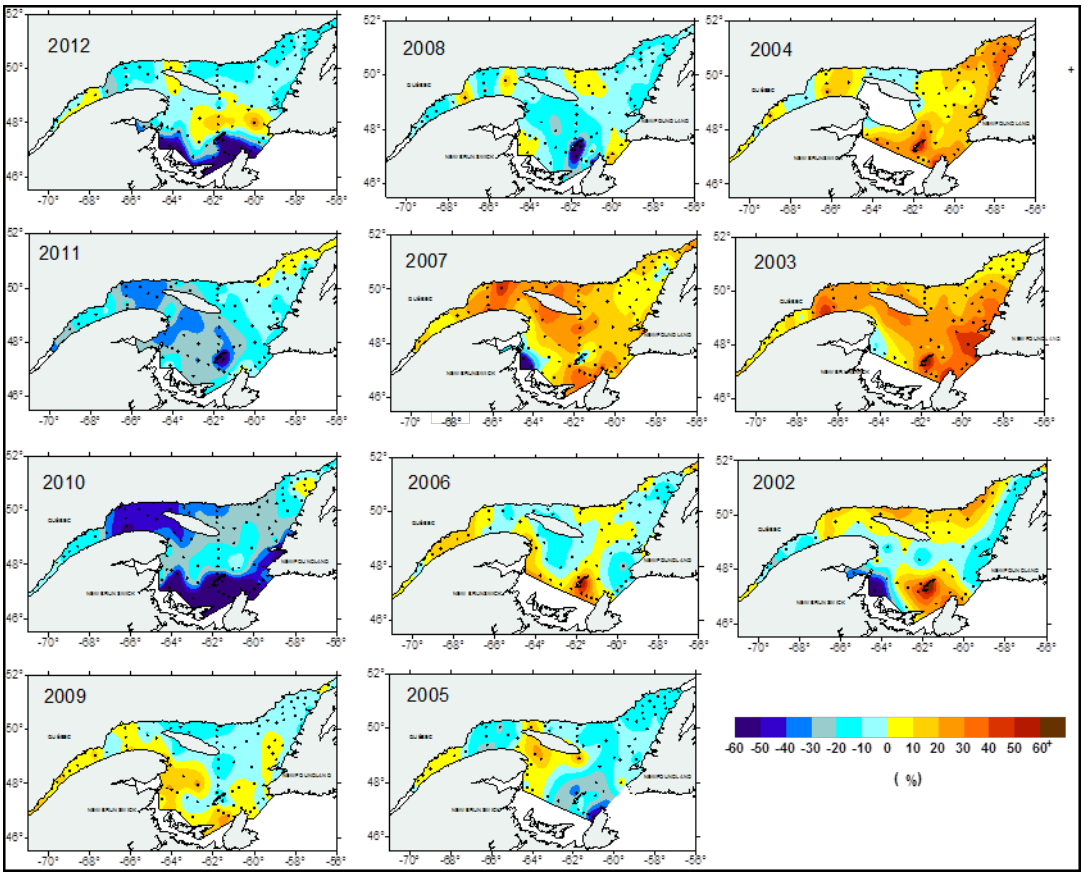

Figure 9. Percentage of change in the late winter (mid-March) nitrate concentrations at 2 m from samples collected during the helicopter survey from 2002 to 2012 relative to the 2001–2010 average. Dots indicate sampling locations.

Index	Transect	1999	2000	2001	2002	2003	2004	2005	2006	2007	2008	2009	2010	2011	2012	Mean	SD
Winter nitrate inventories	TESL			-0.3	-0.6	0.9	0.6		1.5	0.7	-1.5	0.2	-1.5	-1.7	-0.2	770.1	85.5
(0-50m)	TSI			-0.1	0.4	1.2	0.5	-0.8	0.0	1.3	-0.7	0.3	-2.1	-1.2	-0.4	527.7	125.1
(mmol m^{-2})	TASO			-0.2	0.0	1.2	-0.1	0.1	0.3	1.0	-0.1	0.2	-2.5	-1.8	-0.4	521.7	88.6
	TCEN			-0.6	-0.3	1.9	0.8	-0.9	-0.1	1.3	-0.6	-0.6	-0.9	-1.5	0.3	344.3	51.1
	TIDM			0.0	0.4	0.6	0.9	-0.5	0.8	0.5	-0.8	0.4	-2.4	-0.9	-1.3	383.6	98.6
	TBB			-0.3	0.3	1.9	0.9	-0.7	-0.2	0.5	-0.7	0.0	-1.7	-0.5	-0.6	299.0	38.3
	TDC			0.4	0.2	1.3	0.8	-1.0	-0.4	0.7	0.2	0.0	-2.2	-0.4	-1.0	292.5	80.3
Spring nitrate inventories	TESL			0.0	1.7	-0.2	0.4		1.3	-0.8	0.0	-0.9	-1.4	-0.6	0.2	436.8	92.3
(0-50m)	TSI	-1.2	-0.1	1.0	1.4	1.2	-0.7	-0.6	0.0	-0.9	1.5	-0.6	-1.0	-1.0	-0.7	202.6	45.7
(mmol m^{-2})	TASO	-1.5	-0.6	-0.2	1.2	1.7	0.5	-0.7	-0.8	0.8	0.6	0.2	-1.2	-1.0	-1.3	185.6	59.0
	TCEN						-1.5	0.0	1.0	0.0	1.3	0.2	-0.9	-0.9	-1.6	68.2	19.7
	TIDM	-0.8	1.0	-0.8	-0.2	0.3	-0.6	-0.2	1.7	0.0	1.1	0.6	-1.9	-0.5	-1.0	109.4	38.4
	TBB	-0.3	0.3	-0.3	-0.3	2.5	-1.4	-1.0	-0.1	0.7	0.8	-0.6	-0.3	-1.1	-0.8	62.9	23.9
	TDC	-1.2	1.0	-0.2	-1.5	0.8	-0.1	-1.0	0.0	0.6	2.1	0.0	-0.4	-1.5	-0.7	70.7	21.0
Difference between winter	TESL			-0.3	-1.9	0.9	0.1		0.1	1.2	-1.1	1.0	0.0	-0.8	-0.3	332.0	110.6
and late spring nitrate	TSI			-0.4	-0.1	0.9	0.8	-0.5	0.1	1.6	-1.2	0.5	-1.6	-0.8	-0.1	319.4	126.0
(0-50m)	TASO			0.1	-0.8	0.3	-0.3	0.9	1.4	0.9	-0.5	0.3	-2.1	-1.4	0.8	323.3	65.5
(mmol m^{-2})	TCEN						1.4	-0.7	-0.3	1.4	-0.9	-0.5	-0.4	-0.9	1.0	268.8	54.0
	TIDM			0.3	0.6	0.6	1.3	-0.5	0.2	0.6	-1.4	0.1	-1.9	-0.9	-1.1	274.9	83.8
	TBB			-0.1	0.5	0.4	2.0	-0.1	-0.1	0.1	-1.3	0.4	-1.7	0.2	-0.1	236.1	34.8
	TDC			0.5	0.6	1.2	0.9	-0.8	-0.4	0.6	-0.4	0.0	-2.2	0.0	-0.9	221.3	75.0
Fall nitrate inventories	TESL	2.5	-0.1	0.5	1.1	-0.6	-1.1	0.3	-0.8	-0.8	-0.1	-0.6	-0.3	-0.1	0.7	534.5	115.9
(0-50m)	TSI	1.9	-0.7	1.1	1.2	0.5	-1.3	-1.2	-0.3	-0.7	-0.5	-0.3	0.3	-0.5	1.6	268.0	102.2
(mmol m^{-2})	TASO	1.9	-0.3	0.9	1.2	-1.2	-1.0	-0.6	-0.3	-0.6	0.4	-1.0	0.8	-1.0	1.3	277.8	73.5
	TCEN					-0.1	-0.9	-0.4	-0.3	2.1	0.2	0.5	-1.2	-2.8	-1.9	136.1	28.3
	TIDM		1.2	0.6	0.0	-1.2	1.3	0.1	1.3	-0.9	-0.2	-0.9	-1.2	-2.2	-1.3	183.2	36.5
	TBB	0.9	0.3	1.3	0.1	0.8	-1.9	-0.3	-1.6	1.0	-0.4	0.2	-0.5	-0.5	-1.5	125.4	30.5
	TDC	1.4	0.7	-0.2	2.2	-0.6	-1.3	0.1	-0.1	-0.5	-0.6	-0.2	-0.9	-1.0	-0.5	135.5	45.4
Seasonally adjusted nitrate	TESL	2.6	0.1	0.0	1.0	-0.6	-0.6	0.5	-0.1	-0.9	-0.3	-0.9	-0.9	-0.5	0.2	510.7	120.1
inventories (0-50m)	TSI	1.2	-0.6	1.3	1.6	0.9	-1.3	-1.2	-0.3	-0.9	0.2	-0.5	-0.2	-0.8	1.1	235.3	60.4
(mmol m^{-2})	TASO	0.7	-0.8	0.7	2.2	0.2	-0.7	-1.2	-1.0	0.1	0.8	-0.9	-0.2	-1.8	0.3	231.7	35.8
	TCEN					1.2	-1.4	-0.4	0.1	1.1	0.5	0.2	-1.3	-2.3	-2.1	106.3	22.7
	TIDM	-1.8	1.3	0.0	0.0	-0.4	0.5	0.1	1.7	-0.4	0.6	0.0	-1.5	-1.3	-1.1	141.9	35.7
	TBB	0.4	0.4	0.7	-0.1	1.8	-2.0	-0.7	-1.1	1.0	0.1	-0.1	-0.5	-0.9	-1.4	94.2	23.1
	TDC	1.0	1.4	-0.3	1.8	-0.3	-1.6	-0.4	-0.1	-0.3	0.4	-0.3	-1.3	-2.0	-1.0	103.1	19.4
Seasonally adjusted nitrate	TESL			1.0	1.6	0.2	-1.3		0.5	0.0	-0.5	0.1	-1.5	-1.2	1.0	1335.6	110.5
inventories (50-150m)	TSI	0.0	-1.4	0.7	1.2	0.9	-1.4	-0.9	0.7	-0.2	1.3	-1.1	-0.1	-0.5	1.1	1354.4	143.6
(mmol m^{-2})	TASO	-0.1	-1.5	0.2	1.4	0.9	-1.0	-1.0	1.0	-0.1	1.1	0.4	-1.3	-0.5	2.2	1256.1	100.0
	TCEN						-1.5	-0.3	1.2	0.7	0.3	0.7	-1.1	-0.9	-0.3	1092.6	106.3
	TIDM																
	TBB	-2.6	-0.2	0.0	0.5	1.1	-1.0	-0.1	0.9	0.7	0.1	-0.1	0.7	0.4	0.4	897.5	99.0
	TDC	-1.1	1.9	-1.3	0.0	0.3	-1.1	-0.6	1.5	-0.3	0.5	0.4	-0.1	-0.5	1.8	867.0	86.0

Spring chl concentrations	TESL		0.0	1.0	-0.9	1.7	-0.9	0.0	-1.0	1.1	-0.7	-0.1	-0.2	-0.4	-0.1	153.0	97.5
(0-100m)	TSI	-0.2	-1.4	0.1	2.3	-0.3	1.3	-0.8	0.3	0.2	-0.9	-0.7	0.1	-0.3	0.5	69.5	38.0
(mg Chl m^{-2})	TASO	-0.4	-0.7	-0.7	2.8	-0.4	0.5	0.5	0.4	-0.7	-0.6	-0.6	-0.1	-0.6	-0.1	93.6	67.5
	TCEN						-0.8	-0.6	-0.7	0.6	1.7	0.6	-0.8	-0.8	-0.9	38.3	12.0
	TIDM	-0.2	-1.6	-0.5	2.4	0.3	-0.1	-0.7	0.0	-0.2	-0.4	-0.2	1.2	-0.2	-0.3	34.9	13.8
	TBB	-1.0	0.5	-1.2	1.6	-0.8	1.7	-0.7	-0.8	-0.1	0.8	-0.5	0.4	-1.1	-0.4	29.6	10.2
	TDC	2.0	-0.6	0.0	2.1	-0.7	-0.7	-0.7	-0.1	-0.4	-0.5	-0.4	0.1	-0.5	-0.4	47.0	31.8
Fall chl concentrations	TESL	-0.7	-1.6	-0.6	-0.1	1.2	0.2	-0.3	-0.1	0.0	2.4	-0.2	-0.1	-0.4	0.7	23.2	9.0
(0-100m)	TSI	-0.5	-0.9	-0.6	-0.2	0.3	-0.3	0.4	-0.3	-0.2	3.0	-0.5	-0.3	-0.5	-0.3	45.7	33.6
(mg Chl m^{-2})	TASO	-0.6	-1.0	-0.5	-0.2	0.6	-0.5	0.2	-0.1	-0.2	2.9	-0.1	-0.5	-0.3	0.1	45.3	32.1
	TCEN					1.3	-1.4		-0.9	-0.6	0.2	0.3	1.1	-1.5	0.0	41.7	8.3
	TIDM		-1.6	0.6	1.7	0.8	-0.9	-0.9	-0.4	1.2	-0.5	-0.1	0.1	0.5	1.7	38.2	16.5
	TBB	-0.6	-1.4	-0.3	1.4	1.0	2.1	-0.6	-0.7	0.3	-0.6	-0.2	-0.4	1.0	0.8	35.1	10.8
	TDC	-0.9	-1.7	-0.2	1.5	0.4	-0.3	-0.8	0.8	1.1	-0.4	1.3	-0.6	-0.8	-0.7	40.9	11.2
Seasonally adjusted chl	TESL	-1.0	-1.2	1.2	-0.5	1.9	-0.5	-0.9	-0.6	1.3	-0.1	0.2	0.1	-0.1	0.3	70.9	53.5
concentrations (0-100m)	TSI	-0.5	-1.8	-0.4	1.8	-0.1	0.9	-0.4	0.0	0.0	1.5	-1.0	-0.1	-0.6	0.2	57.6	22.3
(mg Chl m^{-2})	TASO	-0.7	-1.1	-0.9	2.6	-0.1	0.3	0.6	0.3	-0.8	0.7	-0.6	-0.4	-0.6	-0.1	69.4	35.9
	TCEN						-1.2	-1.0	-0.9	0.1	1.2	0.5	-0.1	-1.3	-0.6	40.2	9.0
	TIDM	-0.5	-1.5	-0.7	0.9	0.3	-0.2	0.1	-0.2	-0.4	2.5	-0.6	0.4	-0.6	-0.3	36.6	16.2
	TBB	-0.9	-0.5	-0.8	1.7	0.1	2.2	-0.7	-0.9	0.1	0.1	-0.4	0.0	0.0	0.2	32.3	9.2
	TDC	1.5	-1.1	-0.1	2.4	-0.5	-0.7	-0.9	0.1	-0.1	-0.6	0.1	-0.1	-0.7	-0.6	44.0	17.8

Figure 10. *Normalized annual anomalies (scorecard) for nutrient inventories and chlorophyll levels during the winter, late spring, and fall surveys. Blue colours indicate anomalies below the mean and reds are anomalies above the mean.*

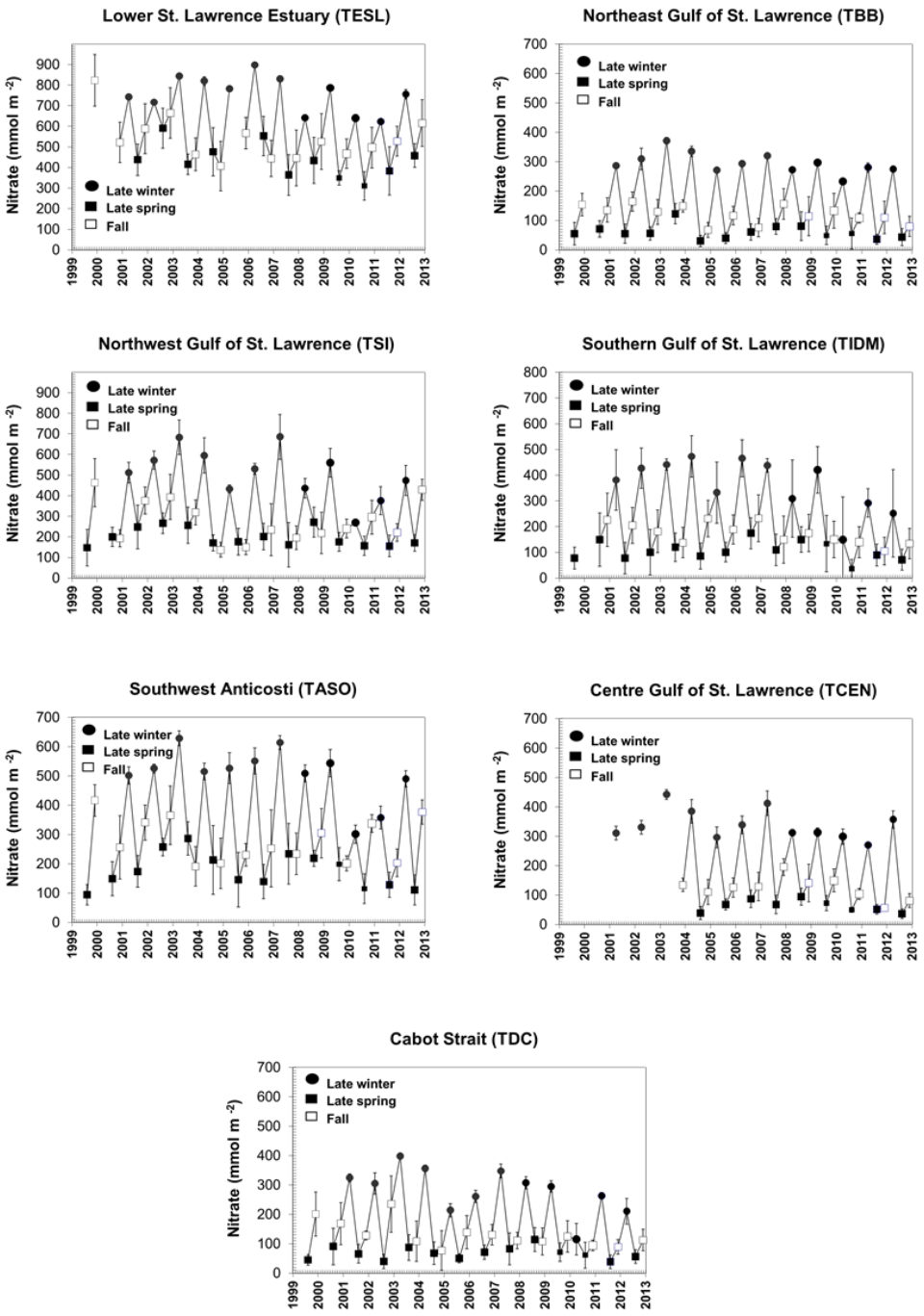

Figure 11. Time series of surface (0–50m) nitrate inventories along the seven AZMP sections from 1999 to 2012. The late winter inventories were calculated using surface concentrations (2 m) × 50 m (assuming that the nitrate concentrations are homogeneous in the winter mixed layer at that time of the year).

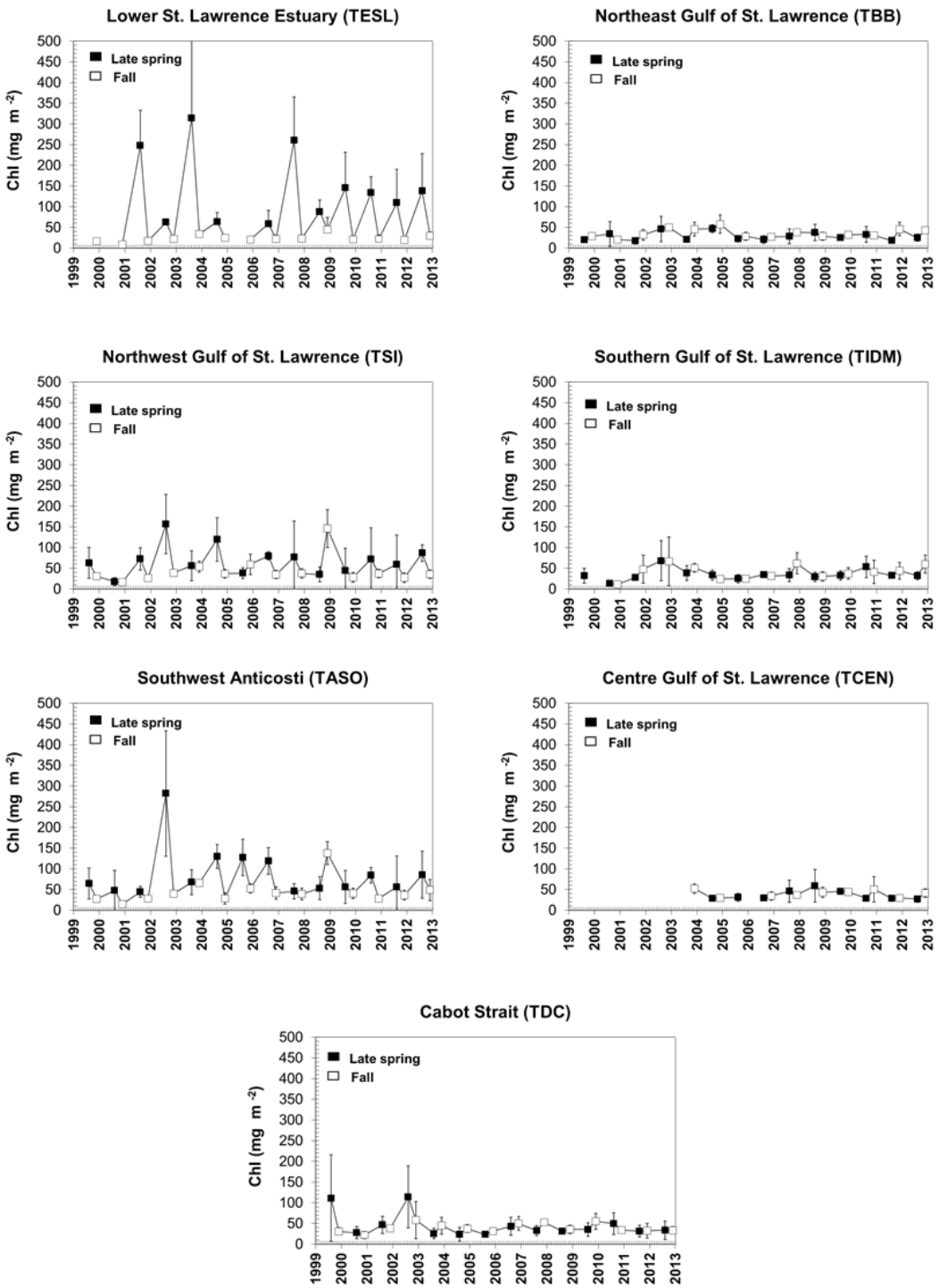

Figure 12. Time series of integrated (0–100 m) chlorophyll biomass along the seven AZMP sections from 1999 to 2012.

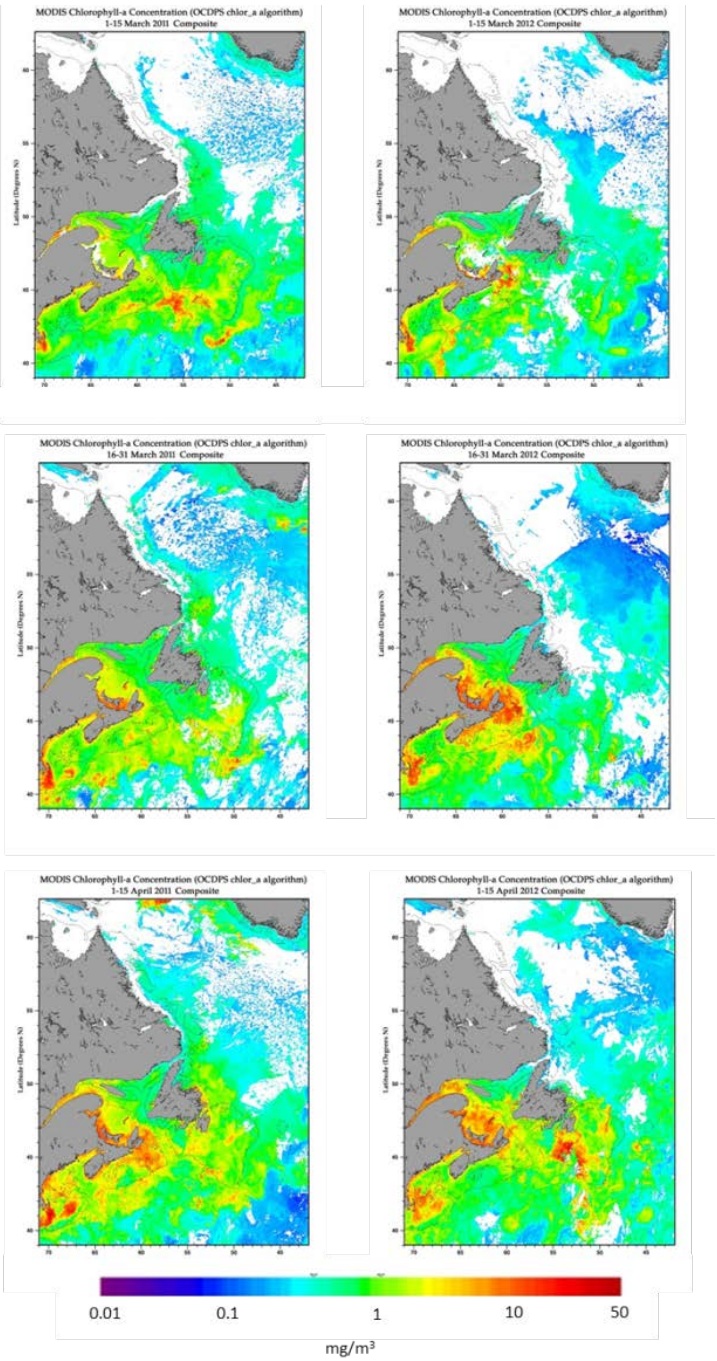

Figure 13. MODIS twice-monthly composite images of surface chlorophyll a in the Gulf of St. Lawrence during late winter – early spring (1–15, 16–31 March; 1–15 April) 2011(left panels) and 2012 (right panel).

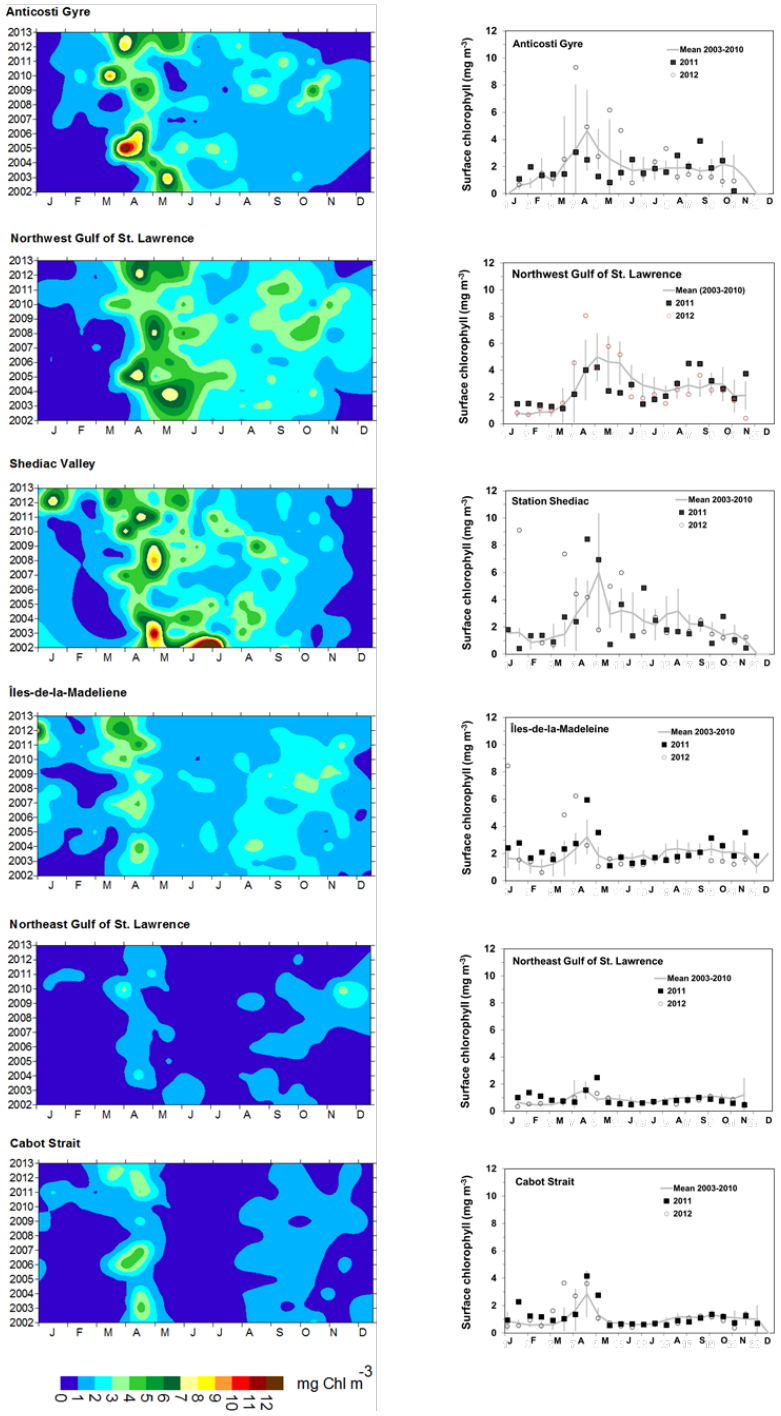

Figure 14. Left panels: Time-series of surface chlorophyll a concentrations from twice-monthly MODIS ocean colour data in the Anticosti Gyre, Northwest Gulf of St. Lawrence, Shediac Valley, Magdalen Shallows, Northeast Gulf of St. Lawrence, and Cabot Strait statistical subregions (see Fig. 3). Right panels: comparison of 2011 (squares) and 2012 (circles) surface chlorophyll estimates from satellite ocean colour with mean conditions from 2003–2010 (solid line) for the same statistical subregions.

Indices of change in productivity based on MODIS twice-monthly ocean colour composites

Index	Subregion	2002	2003	2004	2005	2006	2007	2008	2009	2010	2011	2012
Annual Mean Surface Chl (March to December)	Northwest Gulf of St. Lawrence		-0.69	0.24	1.24	-0.45	-1.82	1.15	0.30	0.03	-0.68	0.15
	Anticosti Gyre		-0.51	-0.52	1.99	-0.49	-1.27	-0.25	0.38	0.68	-0.62	0.89
	Shediac Valley		-0.10	1.40	-1.07	-1.50	-0.53	1.04	0.34	0.41	-0.08	0.03
	Îles-de-la-Madeleine		-1.14	1.34	-1.19	-0.21	-0.01	-0.39	1.51	0.09	1.65	0.27
	Northeast Gulf of St. Lawrence		-0.40	0.14	-0.86	0.12	-0.14	-1.34	0.46	2.01	-0.59	-0.84
	Cabot Strait		-0.17	-0.32	-1.47	1.81	0.82	-0.84	-0.06	0.23	0.31	0.83
Spring bloom magnitude	Northwest Gulf of St. Lawrence		-0.39	1.16	1.34	-0.20	-1.16	0.88	-0.50	-1.14	-1.97	1.08
	Anticosti Gyre		0.86	-0.36	0.60	0.54	-1.45	-1.33	-0.13	1.27	-1.35	0.77
	Shediac Valley		1.62	-0.20	-1.73	-0.72	-0.24	0.81	0.16	0.29	0.33	0.03
	Îles-de-la-Madeleine		-0.52	1.61	-1.50	-0.31	0.64	-0.77	-0.05	0.89	-0.15	2.73
	Northeast Gulf of St. Lawrence		-0.49	0.89	-0.51	-0.25	-0.08	-0.89	-0.76	2.07	0.59	-0.70
	Cabot Strait		1.01	0.26	-1.19	1.18	1.05	-1.10	-0.40	-0.80	0.53	0.21
Mean Surface Chl - March to May	Northwest Gulf of St. Lawrence		-1.33	0.85	1.56	0.42	-1.20	-0.39	-0.34	0.44	-1.00	2.49
	Anticosti Gyre		-0.50	-0.37	2.09	-0.29	-0.93	-0.78	-0.06	0.84	-1.02	1.15
	Shediac Valley		0.43	0.68	-1.55	-1.55	0.87	0.87	0.11	0.14	0.45	0.74
	Îles-de-la-Madeleine		-0.36	0.35	-1.17	-0.28	1.33	-1.31	0.09	1.34	2.08	2.47
	Northeast Gulf of St. Lawrence		-1.25	0.61	-0.53	0.34	0.19	-0.83	-0.47	1.93	0.76	0.29
	Cabot Strait		0.24	-0.18	-1.07	1.79	1.01	-1.16	-0.33	-0.30	0.92	1.79
Mean Surface Chl - June to August	Northwest Gulf of St. Lawrence		0.47	0.67	1.43	-0.16	-1.68	0.66	-0.58	-0.81	-1.63	-1.07
	Anticosti Gyre		-0.05	-0.09	1.98	-0.05	-1.50	0.59	-0.21	-0.67	0.28	0.99
	Shediac Valley		-0.11	1.85	0.42	-0.74	-1.65	-0.16	0.22	0.17	-0.25	-0.46
	Îles-de-la-Madeleine		-0.47	1.92	0.29	0.48	-1.15	0.22	-0.09	-1.19	-1.14	-1.75
	Northeast Gulf of St. Lawrence		1.90	0.63	-0.08	-0.05	-0.65	-1.43	0.31	-0.64	-0.96	-1.30
	Cabot Strait		-0.41	-0.54	-1.59	1.72	0.54	-0.59	0.30	0.57	-1.12	-2.25
Mean Surface Chl - September to December	Northwest Gulf of St. Lawrence	-2.03	-0.40	-1.02	-0.89	-0.90	-0.03	1.46	1.39	0.39	1.36	-0.97
	Anticosti Gyre	-2.11	-0.45	-0.66	-0.60	-1.11	-0.37	0.79	1.95	0.45	0.44	-1.70
	Shediac Valley	0.41	-0.74	-0.78	-1.13	0.17	-0.35	1.96	0.75	0.11	-0.98	-0.84
	Îles-de-la-Madeleine	-1.04	-0.90	0.21	-0.68	-0.33	-0.60	0.57	2.17	-0.45	0.87	-1.07
	Northeast Gulf of St. Lawrence	-0.54	-0.78	-0.72	-0.89	-0.08	-0.02	-0.49	1.02	1.95	-1.12	-0.88
	Cabot Strait	1.23	-1.01	-0.38	-1.67	0.74	-0.10	0.45	0.53	1.42	-0.72	-0.76

Indices of change in seasonality based on MODIS twice-monthly ocean colour composites

Index	Subregion	2002	2003	2004	2005	2006	2007	2008	2009	2010	2011	2012
Start of spring bloom	Northwest Gulf of St. Lawrence		0.76	0.76	0.00	0.00	0.00	0.76	0.00	-2.29	0.00	-0.76
	Anticosti Gyre		1.35	0.75	0.15	0.15	-1.05	0.75	-0.45	-1.65	-2.25	-1.65
	Shediac Valley		0.70	0.70	-0.90	0.70	-0.90	0.70	0.70	-1.70	-0.90	-0.90
	Îles-de-la-Madeleine		0.20	-1.37	-0.59	0.98	0.20	0.98	0.98	-1.37	0.20	-0.59
	Northeast Gulf of St. Lawrence		1.58	0.00	0.00	-1.58	0.00	0.00	-1.58	-3.16	0.00	-1.58
	Cabot Strait		0.98	0.20	0.20	-0.59	0.20	0.98	0.20	-2.15	-3.71	-1.37
Timing of spring bloom peak	Northwest Gulf of St. Lawrence		1.21	1.21	-0.72	-0.72	0.24	0.24	0.24	-1.69	0.24	-0.72
	Anticosti Gyre		1.37	0.53	-0.32	-0.32	0.53	0.53	-0.32	-2.00	-1.16	-1.16
	Shediac Valley		0.78	-0.11	-1.89	-0.11	0.78	0.78	0.78	-1.00	-0.11	-1.89
	Îles-de-la-Madeleine		0.47	0.47	-2.34	0.47	0.47	0.47	0.47	-0.47	1.40	-0.47
	Northeast Gulf of St. Lawrence		2.31	-0.10	-0.10	-0.10	-0.10	-0.10	-0.90	-0.90	0.70	-0.10
	Cabot Strait		0.28	0.28	0.28	-0.85	0.28	1.41	0.28	-1.97	0.28	-1.97

Figure 15. Annual anomalies (scorecard) of chlorophyll biomass indices (means for various time periods and the magnitude of the spring bloom) and indices of seasonality (start and peak timing) of the spring phytoplankton bloom across Gulf of St. Lawrence statistical subregions (based on MODIS twice-monthly ocean colour composites) from 2002 to 2012. The reference period used to compute annual anomalies was 2003–2010. Blue colours indicate anomalies below the mean and reds are anomalies above the mean.

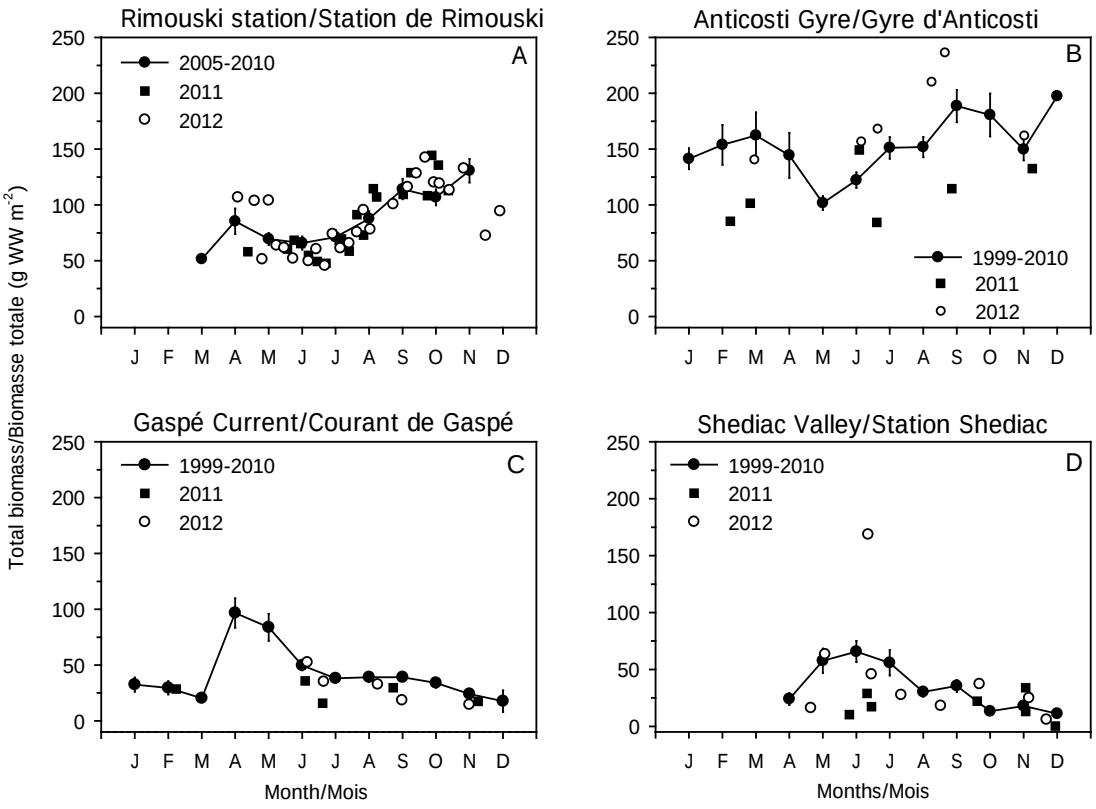

Figure 16. Comparison of total zooplankton biomass in 2011 (squares) and 2012 (circles) with the monthly climatology from 1999–2010 (Rimouski 2005–2010) (solid line) at the Gulf of St. Lawrence fixed stations. Vertical lines are standard errors of the annual averages.

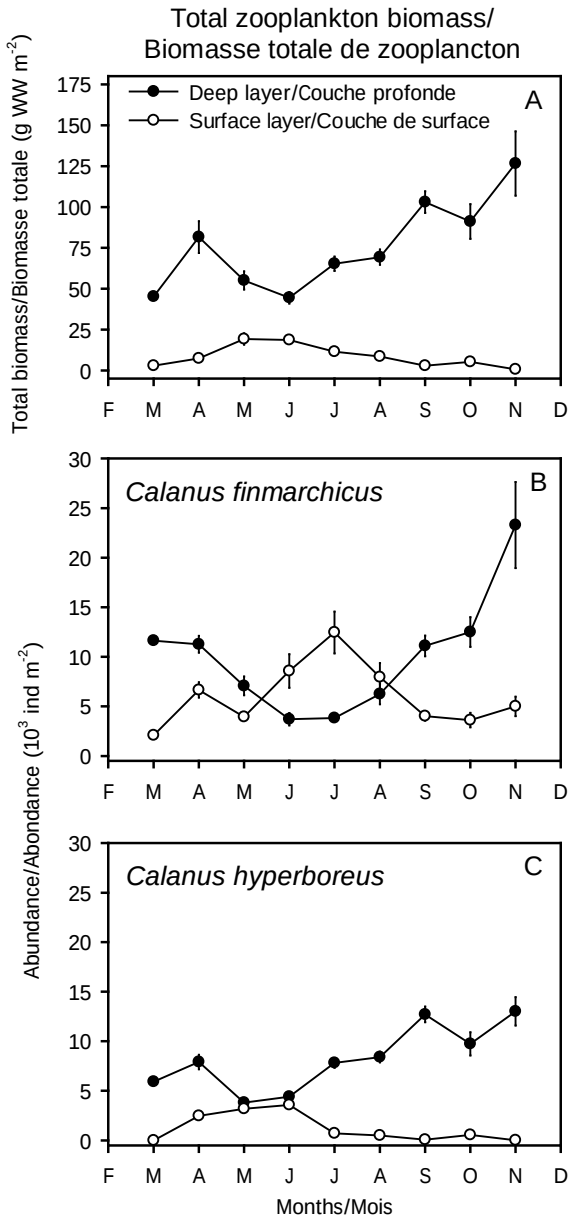

Figure 17. Monthly climatologies of total zooplankton biomass (A) and total abundance of Calanus finmarchicus (B) and Calanus hyperboreus (C) in the surface (0–100 m) and deep (100–320 m) layers at Rimouski station from 2005 to 2010. Vertical lines are standard errors.

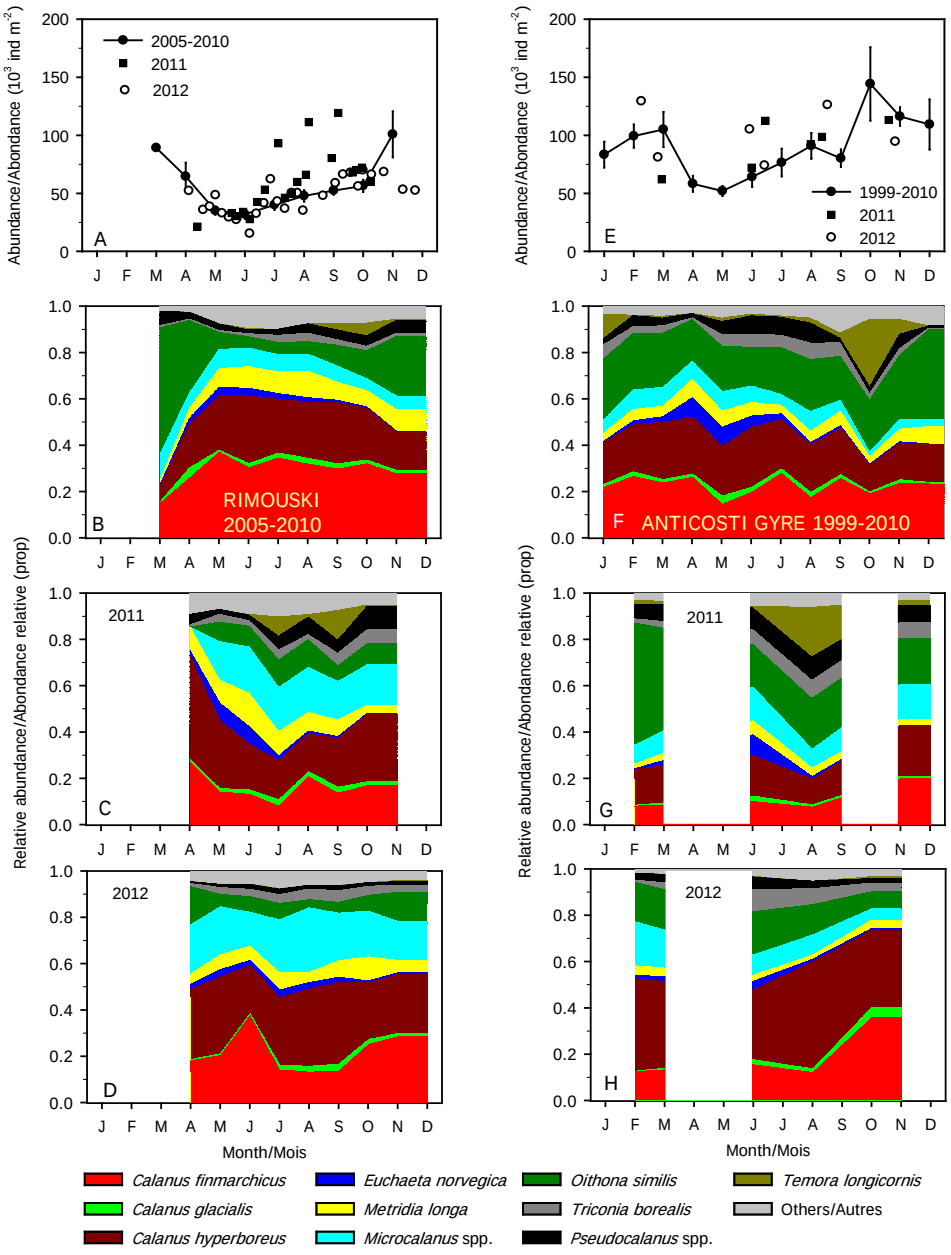

Figure 18. Seasonal variability in abundances of the 10 dominant copepod species at the Rimouski (left panels) and Anticosti Gyre (right panels) fixed stations. Climatologies of combined counts for the reference periods are plotted with data from 2011 (squares) and 2012 (circles)(including the "others" category; A, E). Seasonal variability by species for the reference periods (B, F), for 2011 (C, G), and for 2012 (D, H) are also shown. Vertical bars in A, E are standard errors.

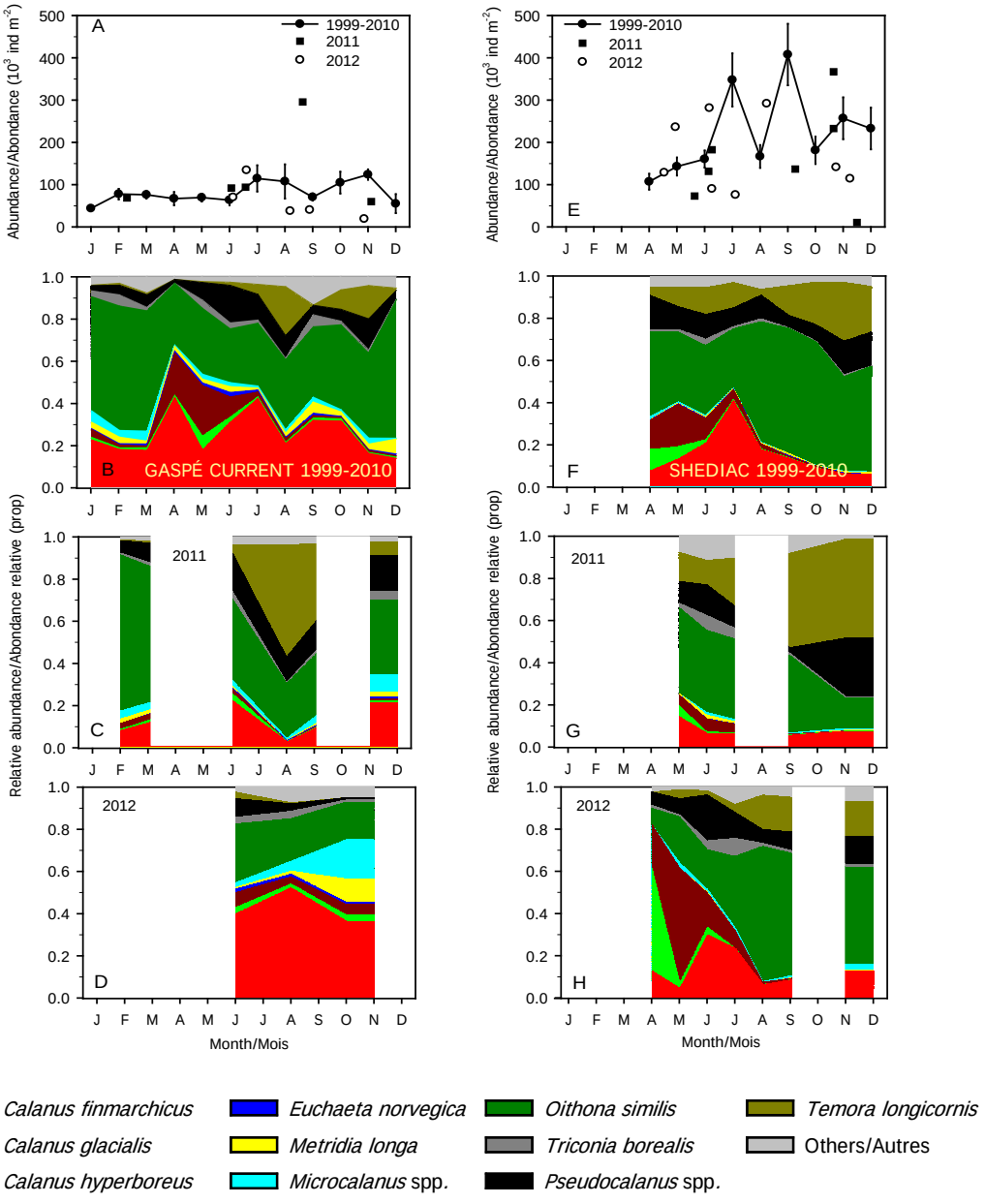

Figure 19. Seasonal variability in abundances of the 10 dominant copepod species at the Gaspé Current (left panels) and Shediac Valley (right panels) fixed stations. Climatologies of combined counts for the reference period are plotted with data from 2011 (squares) and 2012 (circles) (including the "others" category; A, E). Seasonal variability by species for the reference period (B, F), for 2011 (C, G), and for 2012 (D, H) are also shown. Vertical bars in A, E are standard errors.

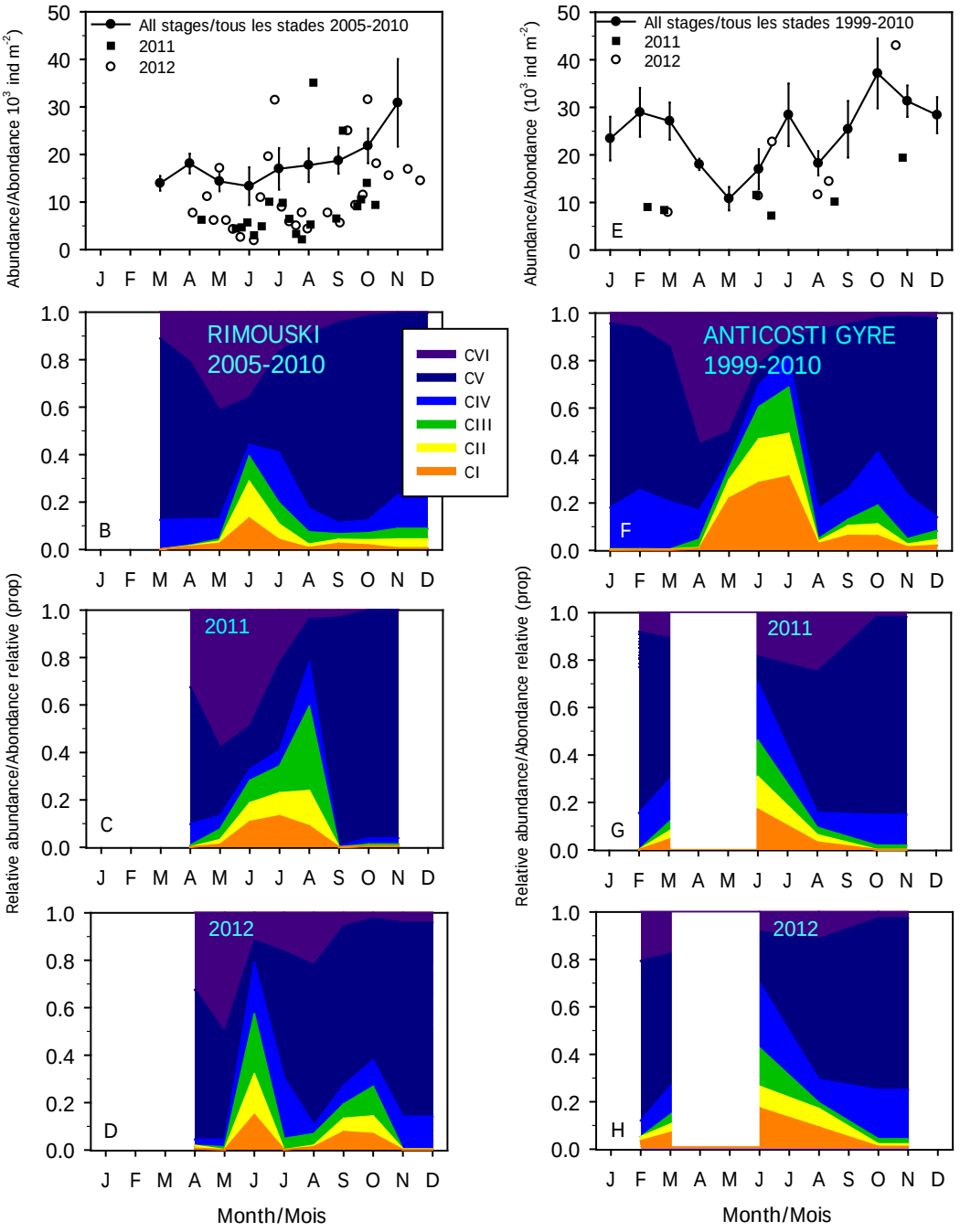

Figure 20. Seasonal variability in Calanus finmarchicus copepodite abundances at the Rimouski (left panels) and Anticosti Gyre (right panels) fixed stations. Climatologies of combined counts for the reference periods are plotted with data from 2011 (squares) and 2012 (circles) (A, E). Seasonal variabilities for the individual copepodite stages for the reference periods (B, F), for 2011 (C, G), and for 2012 (D, H) are also shown. Vertical bars in A, E are standard errors.

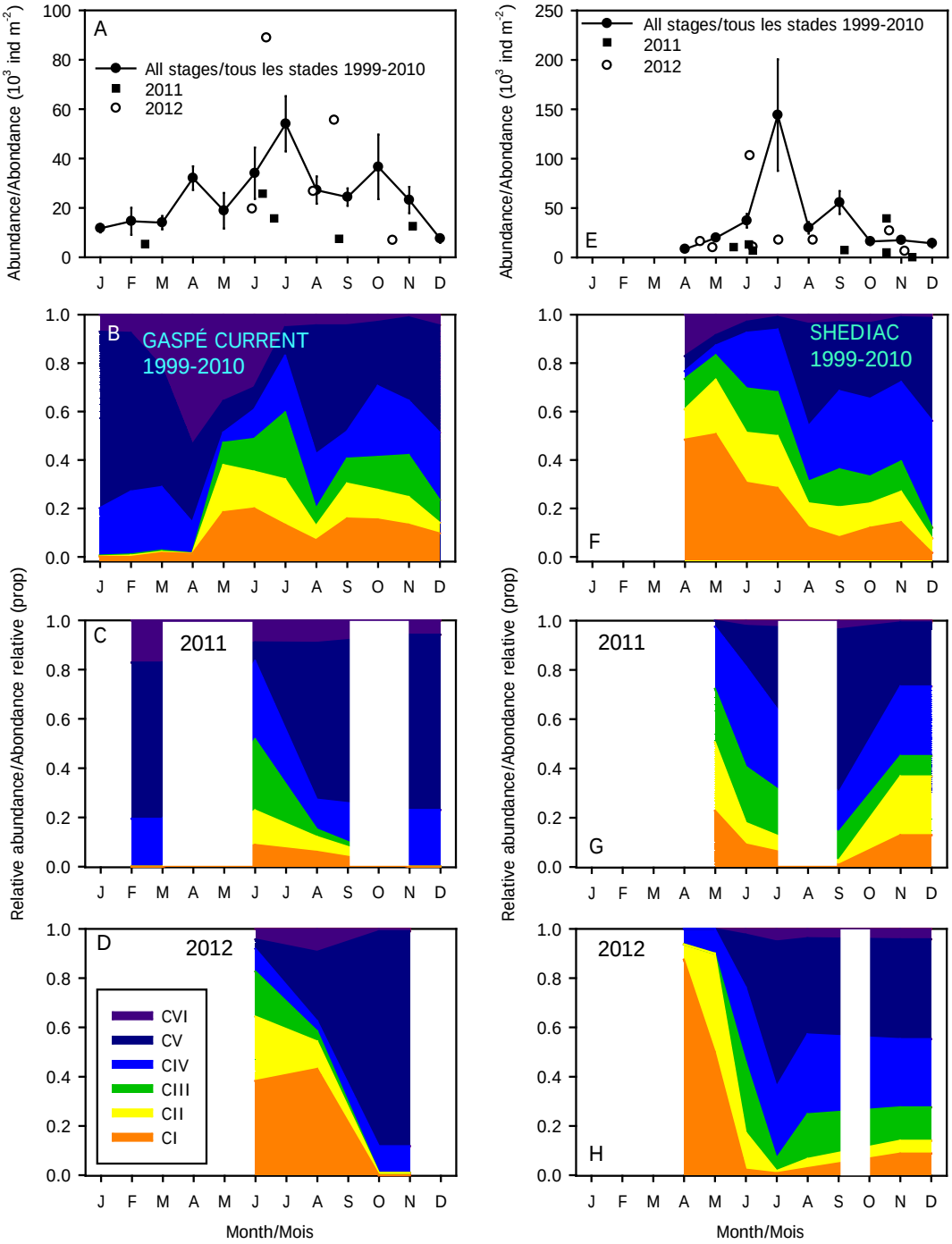

Figure 21. Season variability in Calanus finmarchicus copepodite abundances at the Gaspé Current (left panels) and Shediac Valley (right panels) fixed stations. Climatologies of combined counts for the reference period are plotted with data from 2011 (squares) and 2012 (circles) (A, E). Seasonal variability for the individual copepodite stages for the reference period (B, F), for 2011 (C, G), and for 2012 (D, H) are also shown. Vertical bars in A, E are standard errors.

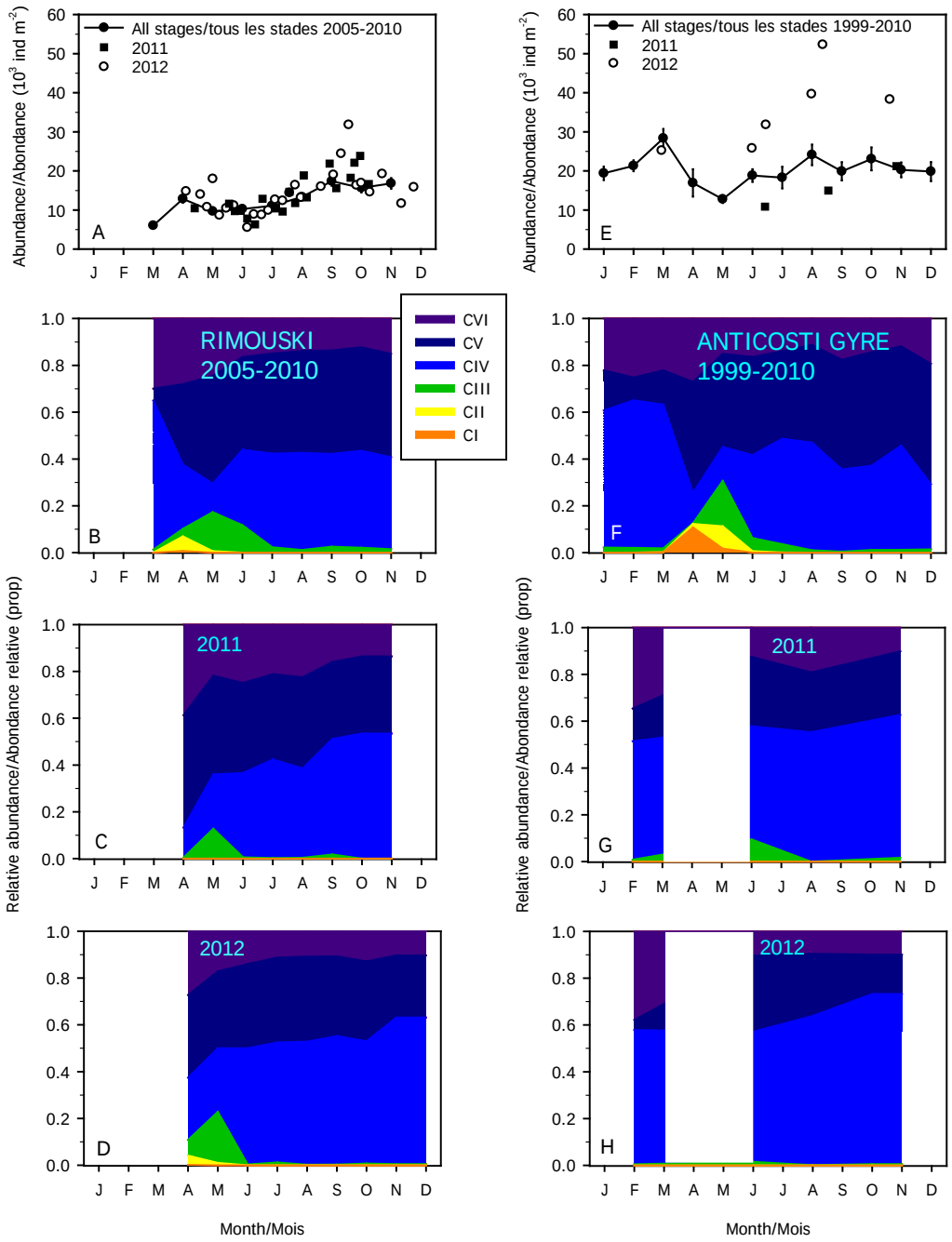

Figure 22. Season variability in Calanus hyperboreus copepodite abundances for the Rimouski (left panels) and Anticosti Gyre (right panels) fixed stations. Climatologies of combined counts for the reference periods are plotted with data from 2011 (squares) and 2012 (circles) (A, E). Seasonal variability for the individual copepodite stages for the reference periods (B, F), for 2011 (C, G), and for 2012 (D, H) are also shown. Vertical bars in A, E are standard errors.

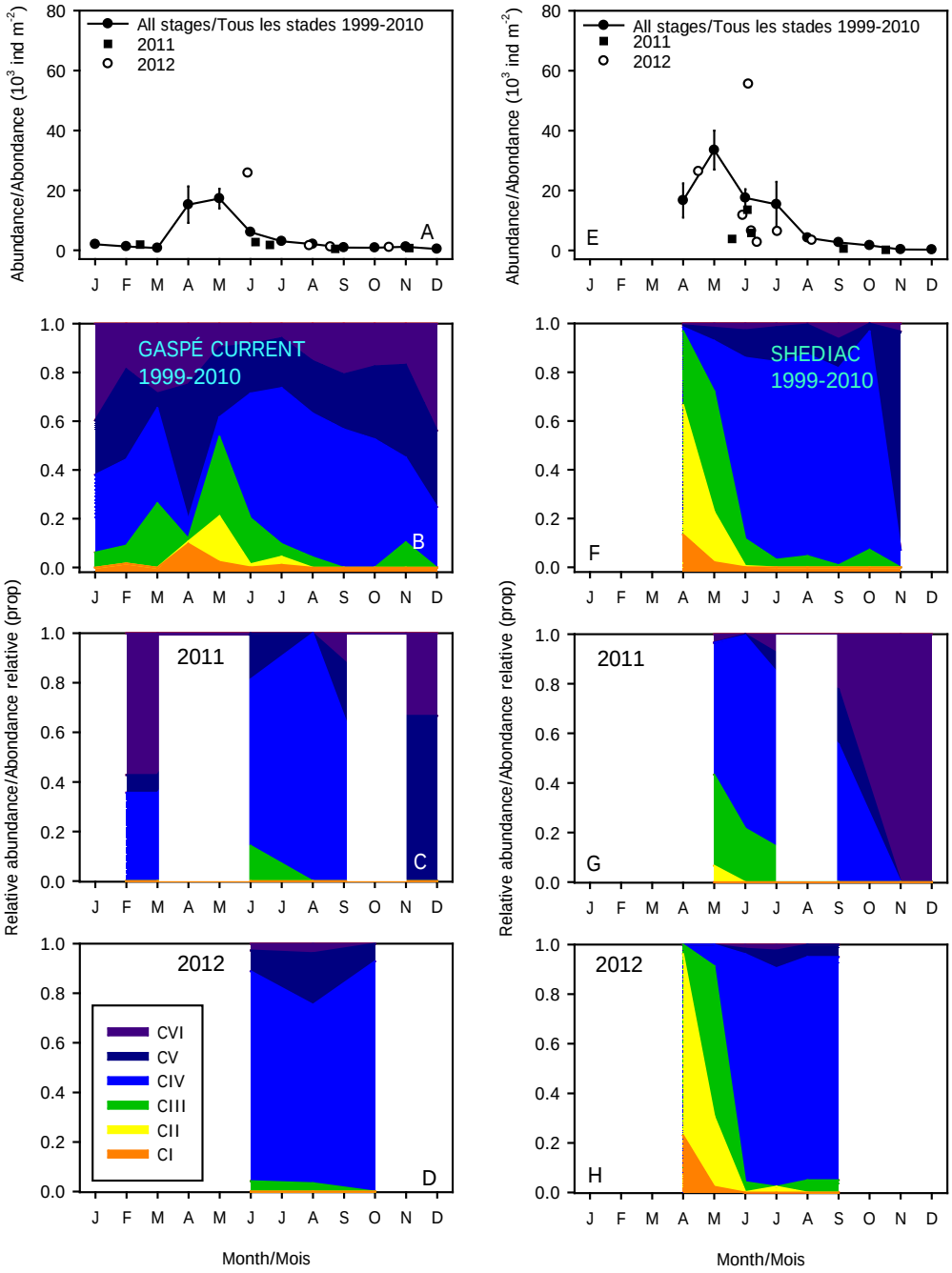

Figure 23. Season variability in Calanus hyperboreus copepodite abundances for the Gaspé Current (left panels) and Shediac Valley (right panels) fixed stations. Climatologies of combined counts for the reference period are plotted with data from 2011 (squares) and 2012 (circles) (A, E). Seasonal variability for the individual copepodite stages for the reference periods (B, F), for 2011 (C, G), and for 2012 (D, H) are also shown. Vertical bars in A, E are standard errors.

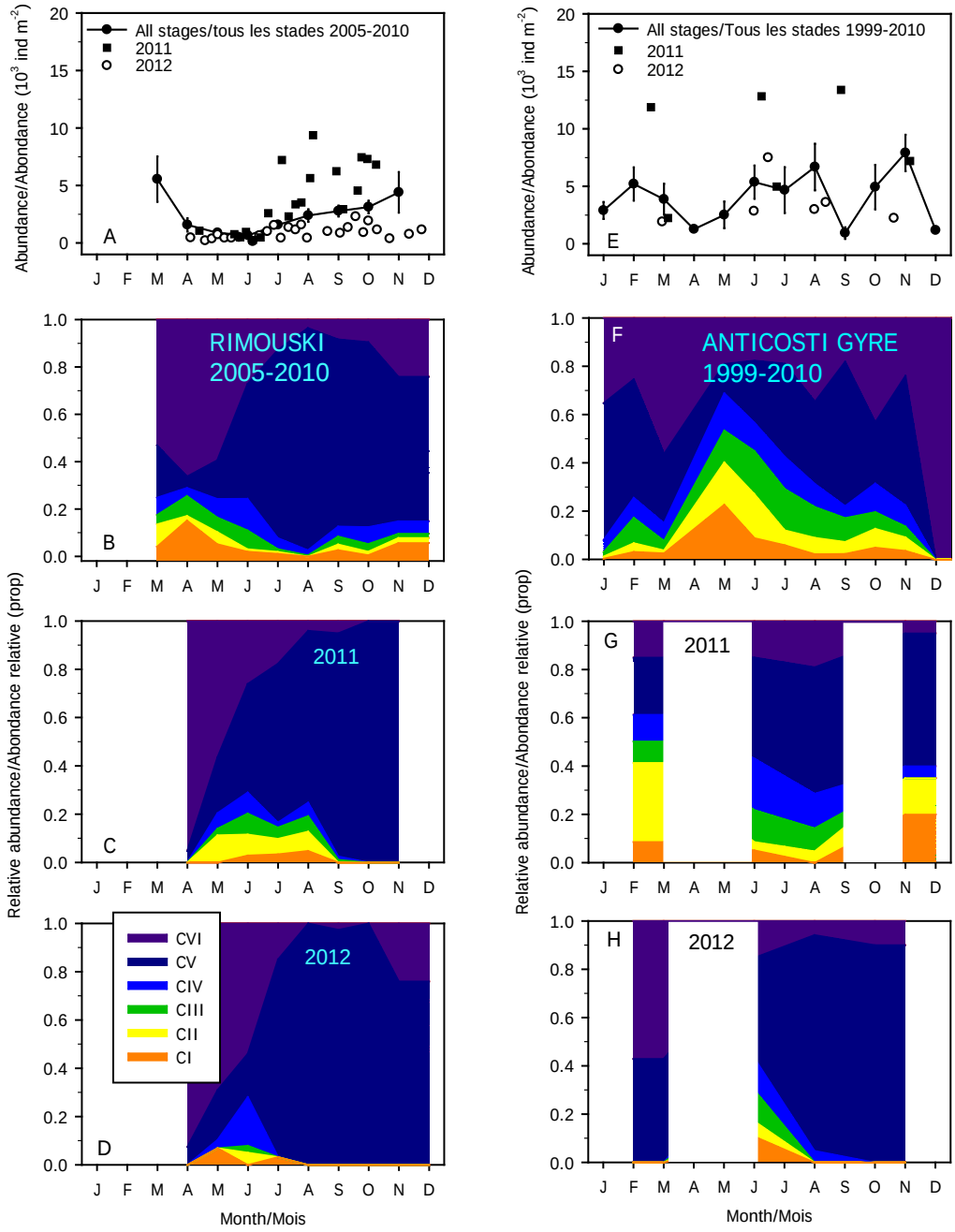

Figure 24. Season variability in Pseudocalanus spp. copepodite stage abundances for the Rimouski (left panels) and Anticosti Gyre (right panels) fixed stations. Climatologies of combined counts for the reference periods are plotted with data from 2011 (squares) and 2012 (circles) (A, E). Seasonal variability and for the individual copepodite stages for the reference periods (B, F), for 2011 (C, G), and for 2012 (D, H) are also shown. Vertical bars in A, E are standard errors.

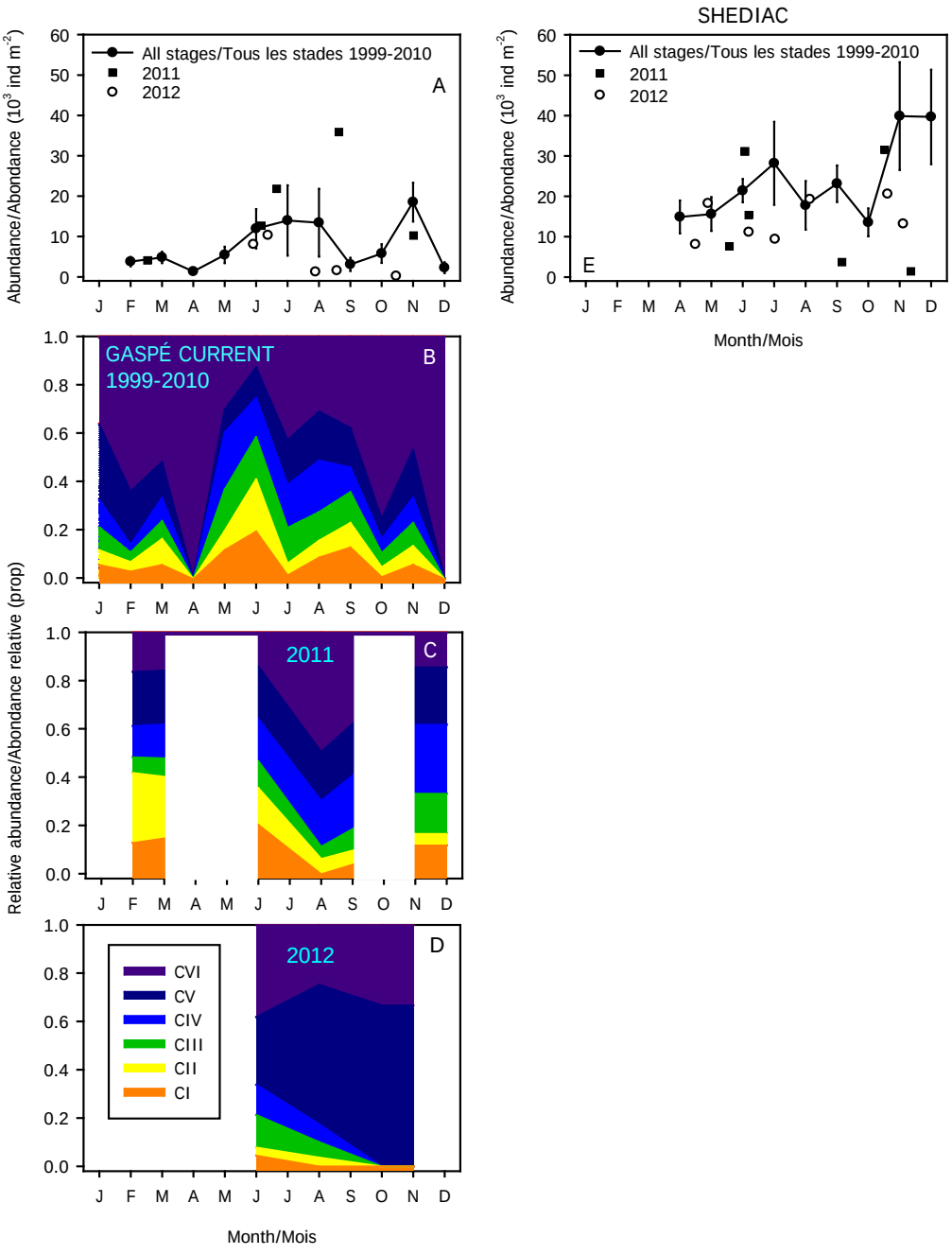

Figure 25. Season variability in Pseudocalanus spp. copepodite stage abundances for the Gaspé Current (left panels) and Shediac Valley (right panel) fixed stations. Climatologies of combined counts for the reference period are plotted with data from 2011 (squares) and 2012 (circles) (A, E). Seasonal variability for the individual copepodite stages for the reference period (B), for 2011 (C), and for 2012 (D) at the Gaspé Current are also shown; no stage information is available for Shediac Valley. Vertical bars in A, E are standard errors.

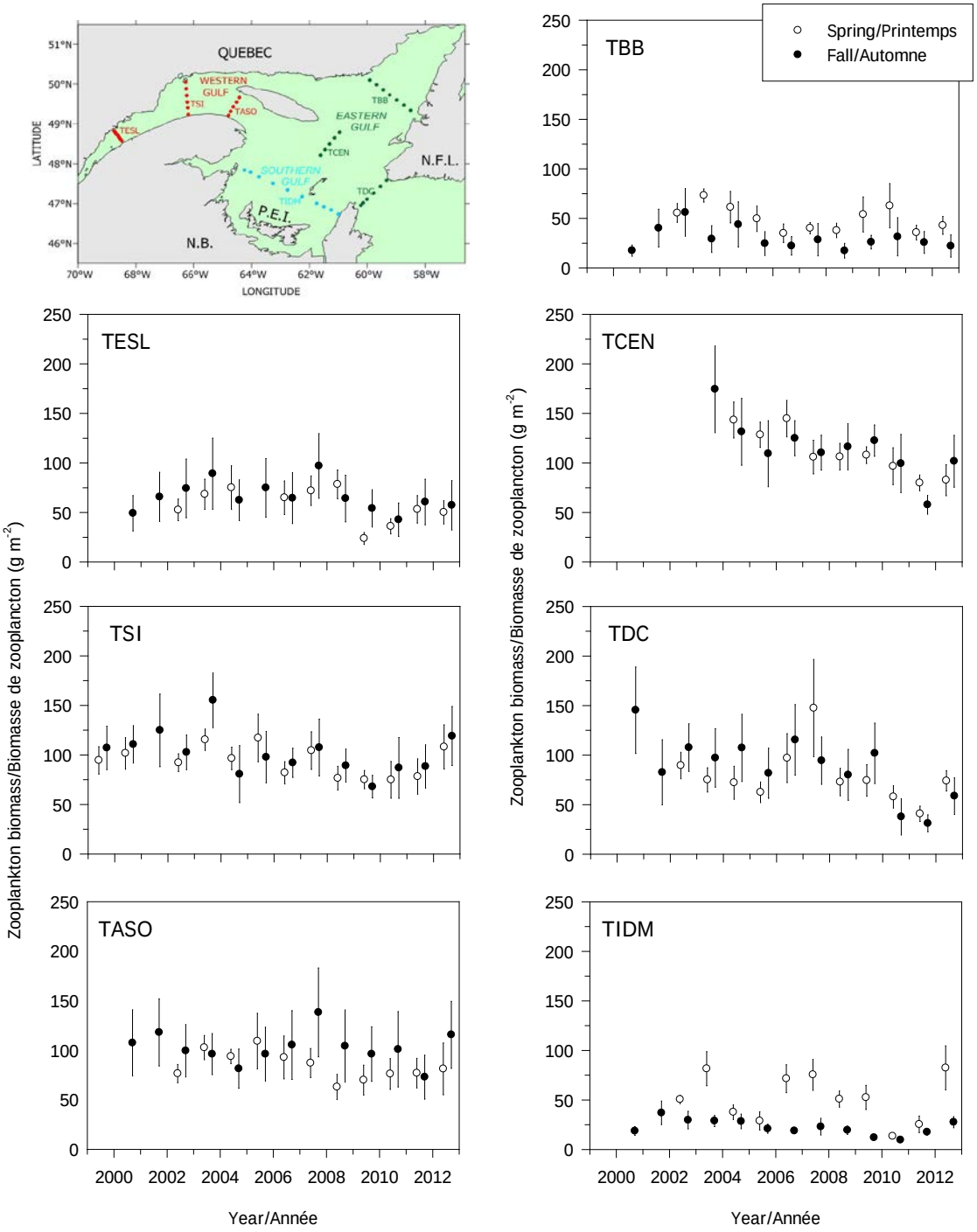

Figure 26. Mean total zooplankton biomass for the seven Estuary and Gulf of St. Lawrence sections during spring and fall from 1999 to 2012. Vertical bars represent standard errors.

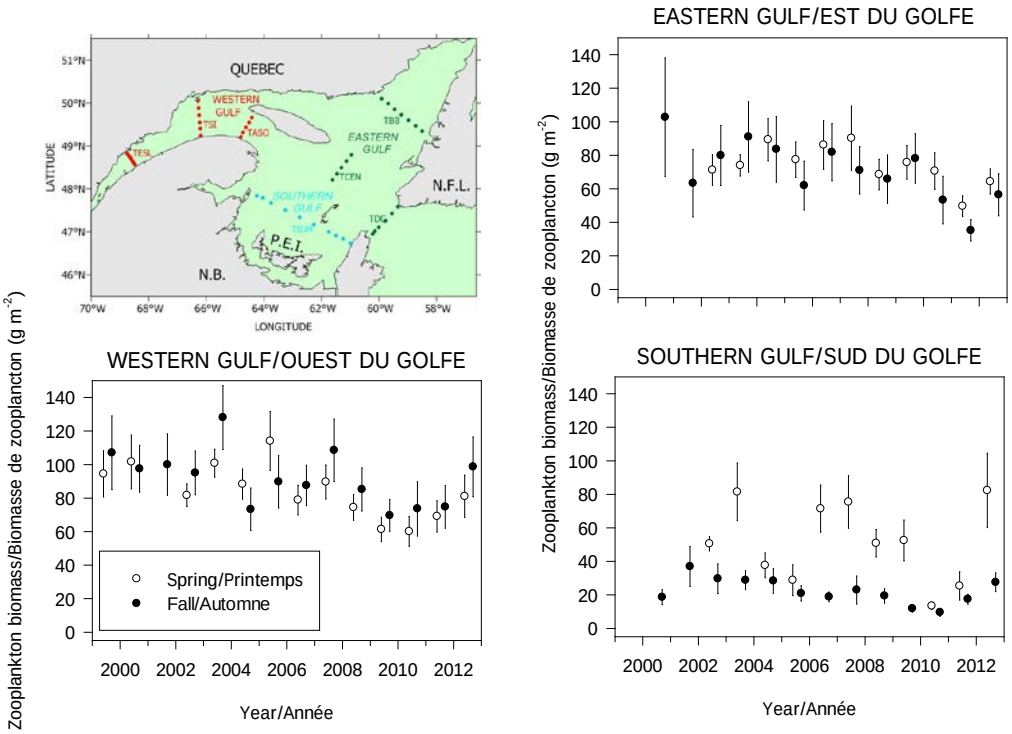

Figure 27. Mean total zooplankton biomass during spring and fall for three subregions of the Estuary and Gulf of St. Lawrence from 1999 to 2012. Vertical bars represent standard errors.

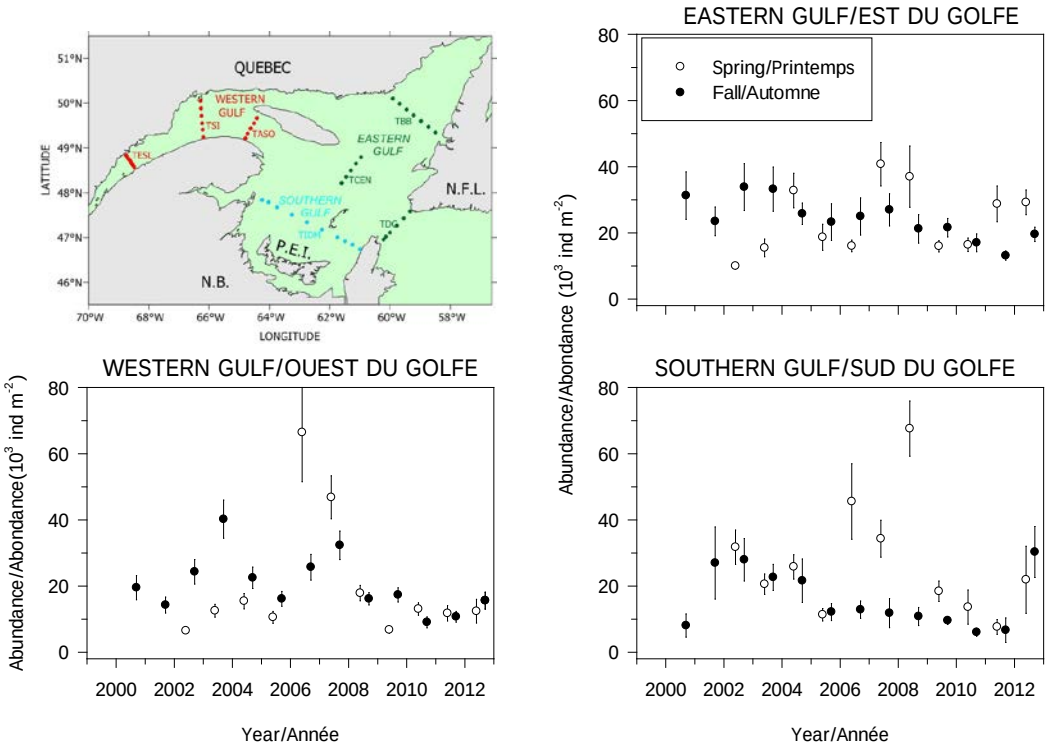

Figure 28. Mean total abundance of Calanus finmarchicus during spring and fall for three subregions of the Estuary and Gulf of St. Lawrence from 1999 to 2012. Vertical bars represent standard errors.

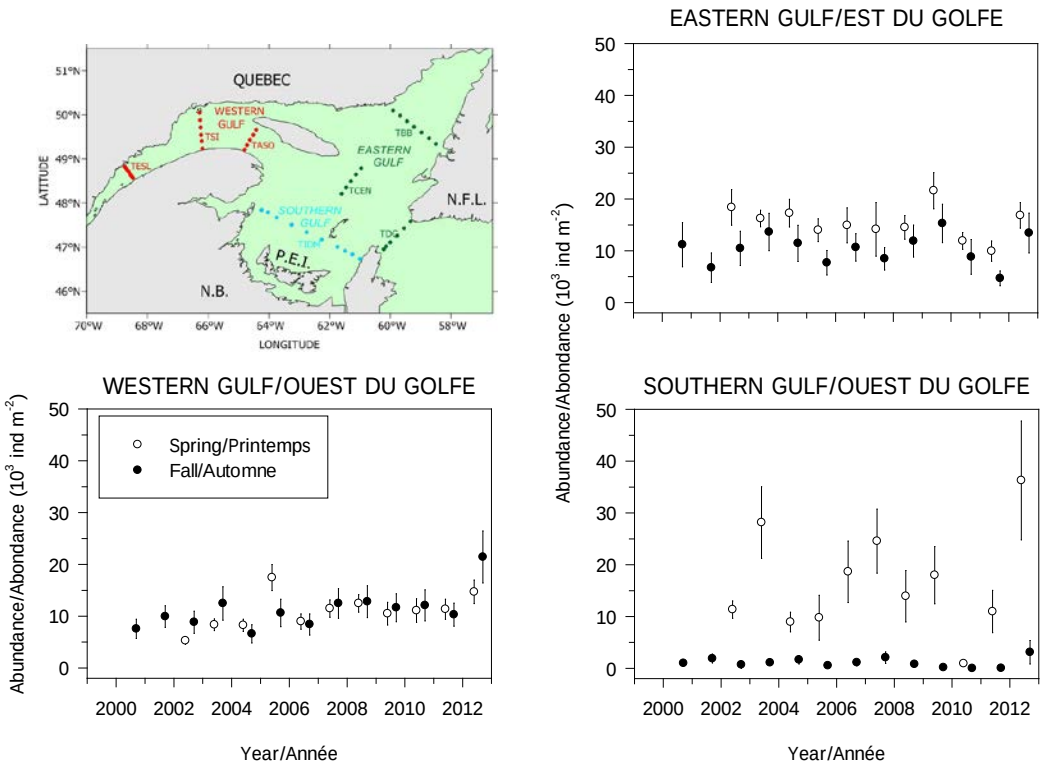

Figure 29. Mean total abundance of Calanus hyperboreus during spring and fall for three subregions of the Estuary and Gulf of St. Lawrence from 1999 to 2012. Vertical bars represent standard errors.

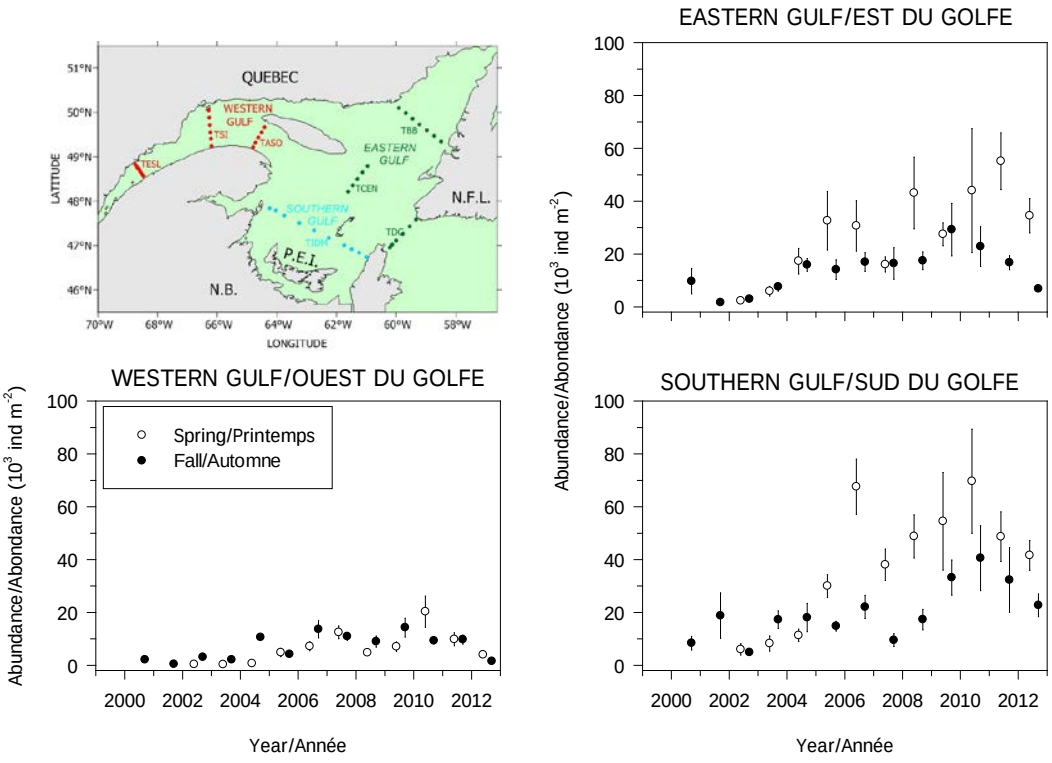

Figure 30. Mean total abundance of Pseudocalanus spp. during spring and fall for three subregions of the Estuary and Gulf of St. Lawrence from 1999 to 2012. Vertical bars represent standard errors.

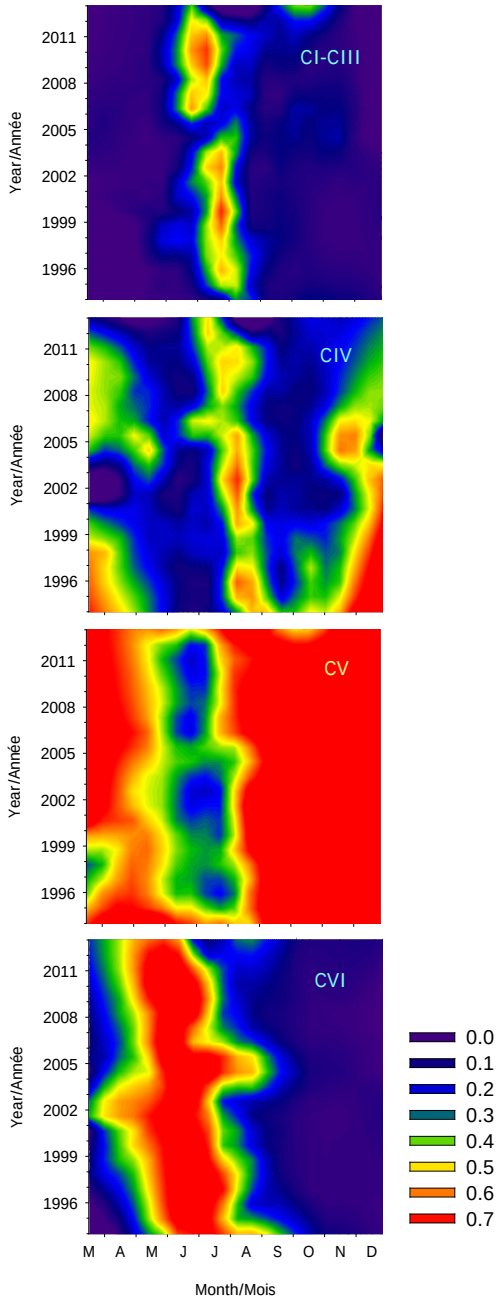

Figure 31. Seasonal cycle in proportions (proportion of stage-specific annual maximum) of stage CI–III, CIV, CV, CVI (male + female) Calanus finmarchicus copepodites from 1994 to 2012 at Rimouski station.

	Regions	1999	2000	2001	2002	2003	2004	2005	2006	2007	2008	2009	2010	2011	2012
C. finmarchicus	Rimouski							-1.01	-0.11	1.72	0.39	-0.08	-0.92	-0.66	-0.57
	Gaspé Current	-0.41	-0.54	-1.56	-0.03	1.73	0.12	-0.97	0.12	1.19	0.22	1.21	-1.09	-0.78	0.37
	Anticosti Gyre	-1.12	-0.97	0.06	-0.83	2.28	1.35	-0.27	0.58	0.05	-0.08	-0.32	-0.74	-1.66	-0.72
	Shediac	-0.62	-0.21	-0.32	-0.44	2.58	1.27	-0.37	0.03	-0.14	0.12	-1.01	-0.90	-1.29	-0.05
	TESL		-0.07	-0.77	0.16	0.42	0.04	-0.19	-0.20	2.66	-0.12	-0.70	-1.24	-1.10	-1.03
	TSI		0.03	-0.26	-0.79	1.13	-0.12	-0.90	2.02	1.17	-0.56	-0.85	-0.86	-0.71	-0.66
	TASO		-0.21	-0.63	-0.51	-0.03	-0.33	-0.54	2.65	1.04	-0.28	-0.63	-0.54	-0.67	-0.24
	TIDM		-1.43	0.54	0.86	-0.02	0.23	-1.04	0.80	0.14	1.82	-0.81	-1.08	-1.53	0.45
	TCEN					1.91	-0.58	-0.62	-0.43	1.17	-0.05	-0.49	-0.92	-0.76	-0.02
	TBB		-0.37	0.14	-0.59	-0.87	1.10	-0.10	-1.19	1.09	2.03	-0.71	-0.53	-0.27	0.50
	TDC		1.88	-0.26	0.20	-0.22	1.79	-0.50	0.05	-0.31	-0.38	-0.98	-1.28	0.17	-0.78
	wGSL		-0.16	-0.61	-0.51	0.47	-0.23	-0.63	2.14	1.59	-0.37	-0.80	-0.89	-0.87	-0.63
	sGSL		-1.43	0.54	0.86	-0.02	0.23	-1.04	0.80	0.14	1.82	-0.81	-1.08	-1.53	0.45
	eGSL		1.29	-0.18	-0.47	0.16	0.98	-0.66	-0.86	1.38	0.88	-1.06	-1.46	-0.61	0.00
Pseudocalanus spp.	Rimouski							-1.06	-0.79	0.69	-0.50	0.07	1.59	1.78	-0.94
	Gaspé Current	-0.75	-0.67	-0.88	-0.86	-0.73	-0.57	-0.34	-0.14	0.45	0.99	1.50	2.01	0.58	-0.57
	Anticosti Gyre	-0.90	-0.97	-0.89	-0.92	-0.82	0.14	-0.13	-0.17	0.39	0.79	1.74	1.75	0.71	-0.38
	Shediac	1.34	-0.85	1.92	-0.07	-0.11	-0.96	0.42	-1.50	-0.81	-0.31	0.12	0.81	0.98	-0.17
	TESL		-0.64	-1.15	-1.15	-0.92	1.23	-0.64	1.42	1.28	-0.27	0.20	0.64	0.07	-0.80
	TSI		-0.80	-0.99	-0.84	-0.97	-0.50	-0.41	0.56	0.71	0.02	1.17	2.04	0.31	-0.62
	TASO		-0.83	-1.32	-0.76	-0.96	-0.47	-0.50	0.85	1.55	0.51	0.56	1.39	1.66	-0.67
	TIDM		-1.02	-0.43	-1.18	-0.77	-0.68	-0.22	1.06	-0.14	0.39	1.00	2.00	0.81	0.34
	TCEN					-1.23	-0.95	-1.36	0.66	0.29	0.80	0.90	0.88	4.20	1.33
	TBB		-1.04	-1.12	-1.10	-0.86	-0.31	0.17	0.15	0.18	1.40	1.70	0.83	1.29	0.62
	TDC		-0.71	-1.30	-1.19	-0.89	0.05	0.79	0.78	-0.41	0.77	0.22	1.89	1.35	-0.17
	wGSL		-0.86	-1.20	-0.94	-1.04	-0.23	-0.38	0.83	1.10	0.11	0.88	1.72	0.71	-0.73
	sGSL		-1.02	-0.43	-1.18	-0.77	-0.68	-0.22	1.06	-0.14	0.39	1.00	2.00	0.81	0.34
	eGSL		-0.70	-1.41	-1.33	-0.95	-0.08	0.53	0.55	-0.12	1.12	0.96	1.43	1.67	0.27
Total copepods	Rimouski							-1.47	-0.62	1.14	-0.19	1.05	0.08	1.38	-0.10
	Gaspé Current	1.14	-0.79	-1.34	-1.26	-0.19	-0.69	0.00	-0.52	0.06	1.35	0.60	1.65	0.26	-1.25
	Anticosti Gyre	1.78	-1.37	-0.41	-1.51	-0.05	0.38	0.10	-0.54	-0.66	1.52	0.43	0.34	-0.12	-0.37
	Shediac	0.72	-0.95	-0.34	-0.72	1.24	0.03	-0.33	-0.99	0.69	2.13	-1.07	-0.41	-0.69	-0.85
	TESL		-0.60	-1.00	-1.48	-1.14	-0.04	0.63	0.22	1.94	0.32	0.31	0.85	-0.77	-1.78
	TSI		0.83	-0.43	-1.30	-1.18	-0.80	-0.83	0.82	0.18	0.79	0.08	1.84	-0.61	-1.55
	TASO		-0.36	-1.22	-0.48	-1.01	-0.63	-0.60	2.07	-0.09	1.09	0.30	0.92	-0.21	-1.05
	TIDM		-1.41	-0.19	0.67	-0.60	-0.47	-1.61	0.76	-0.19	1.54	1.11	0.39	-0.07	0.16
	TCEN					1.51	-0.69	-1.30	-0.68	0.00	-0.06	-0.21	1.43	0.39	-0.28
	TBB		1.73	-1.45	-0.15	-0.66	1.41	-0.53	-1.33	0.10	0.49	0.41	-0.01	0.55	-0.38
	TDC		2.29	-1.35	0.09	-0.27	0.50	-0.95	0.42	-0.68	0.79	-0.62	-0.22	0.50	-1.32
	wGSL		-0.16	-0.99	-1.18	-1.28	-0.66	-0.37	1.37	0.58	0.95	0.27	1.48	-0.56	-1.65
	sGSL		-1.41	-0.19	0.67	-0.60	-0.47	-1.61	0.76	-0.19	1.54	1.11	0.39	-0.07	0.16
	eGSL		2.51	-1.25	0.02	-0.21	0.58	-0.97	-0.74	-0.28	0.33	-0.20	0.22	0.41	-0.79
Non copepods	Rimouski							-0.93	-0.70	1.15	-0.97	0.31	1.13	2.65	-1.07
	Gaspé Current	0.09	0.38	-1.04	-0.63	-0.38	-0.99	-0.77	-0.13	1.66	2.13	0.23	-0.56	1.97	-0.17
	Anticosti Gyre	0.74	-0.25	-1.22	-0.96	-0.86	-1.04	-0.39	1.02	1.52	0.75	1.31	-0.62	0.95	-0.85
	Shediac	1.70	-0.94	0.42	-0.26	-1.25	-0.79	1.04	0.24	0.27	1.34	-1.22	-0.55	-0.06	3.52
	TESL		-0.40	-0.56	-0.60	0.52	-0.52	-0.58	-0.09	2.85	-0.38	-0.17	-0.06	-0.23	-0.42
	TSI		-0.69	-0.90	-0.74	-0.05	-0.70	-0.61	2.33	1.33	0.17	-0.25	0.11	1.45	-0.49
	TASO		-0.56	-0.80	-0.66	-0.72	-0.67	-0.61	0.98	2.11	1.33	-0.06	-0.35	1.41	0.16
	TIDM		-0.75	-0.89	-0.24	-0.65	-0.75	0.64	-0.20	0.02	0.06	0.11	2.67	1.63	1.39
	TCEN					-1.68	-0.03	0.29	1.66	0.86	-0.03	-0.67	-0.40	4.13	-0.36
	TBB		1.27	-1.98	0.32	-1.27	0.07	0.73	1.35	0.04	0.02	0.06	-0.61	6.87	0.87
	TDC		-0.97	-1.42	-1.01	-0.81	0.14	1.91	0.87	0.89	-0.08	0.19	0.29	2.74	-0.87
	wGSL		-0.65	-0.89	-0.77	-0.19	-0.75	-0.62	1.39	2.23	0.53	-0.18	-0.12	1.16	-0.28
	sGSL		-0.75	-0.89	-0.24	-0.65	-0.75	0.64	-0.20	0.02	0.06	0.11	2.67	1.63	1.39
	eGSL		-0.37	-1.83	-0.63	-1.06	0.24	1.68	1.23	0.77	-0.02	0.07	-0.06	4.43	-0.35

Figure 32. Normalized annual anomalies (scorecard) for four zooplankton categories. Blue colours indicate anomalies below the mean and reds are anomalies above the mean.

	Regions	1999	2000	2001	2002	2003	2004	2005	2006	2007	2008	2009	2010	2011	2012
C. hyperboreus	Rimouski							0.81	-0.09	0.18	1.32	-1.27	-0.97	0.72	0.85
	Gaspé Current	0.10	-0.27	-1.39	-0.11	1.89	-0.61	0.00	-0.40	-0.51	1.06	1.43	-1.20	-0.94	0.00
	Anticosti Gyre	-0.89	0.08	0.32	-1.94	0.14	0.23	1.26	-0.40	-0.26	-0.68	0.15	1.99	-0.89	3.48
	Shediac	0.16	0.76	-0.52	-1.32	1.15	-0.74	1.81	1.14	-0.14	-1.10	-0.73	-0.45	-1.13	2.24
	TESL		-0.86	-0.19	-0.99	-0.09	-0.49	0.99	0.00	0.89	2.24	-0.95	-0.54	0.49	1.69
	TSI		-0.78	-0.32	-1.33	1.33	-1.12	0.35	-1.02	0.62	0.49	0.15	1.64	1.07	5.15
	TASO		-0.91	0.25	-1.21	-0.54	-1.21	1.09	-0.70	0.61	0.10	1.82	0.71	-0.65	2.71
	TIDM		-1.24	-1.05	-0.11	1.67	-0.24	-0.36	0.66	1.39	0.12	0.49	-1.32	-0.28	2.76
	TCEN					0.16	0.58	0.01	-0.12	-1.80	0.29	1.64	-0.76	-1.05	-0.04
	TBB		-1.50	-1.02	1.10	1.21	1.20	-0.41	-0.75	-0.63	-0.64	0.84	0.59	-0.42	0.55
	TDC		0.31	-1.17	0.96	0.41	-0.52	-1.02	0.49	1.29	0.21	0.89	-1.85	-2.44	0.77
	wGSL		-1.20	-0.09	-1.42	0.15	-1.22	1.38	-0.67	0.83	1.15	0.43	0.67	0.31	3.70
	sGSL		-1.24	-1.05	-0.11	1.67	-0.24	-0.36	0.66	1.39	0.12	0.49	-1.32	-0.28	2.76
	eGSL		-0.47	-1.94	0.59	0.71	0.66	-0.56	0.05	-0.41	0.19	1.91	-0.73	-1.73	0.83
Small calanoids	Rimouski							-0.86	-0.42	1.66	0.77	-0.34	-0.80	1.22	0.21
	Gaspé Current	-0.68	-0.79	-1.60	-0.72	0.39	-0.33	-0.80	0.26	0.60	1.65	1.62	0.39	1.18	-0.23
	Anticosti Gyre	-1.38	-0.97	-0.51	-1.67	0.43	0.48	0.18	0.10	0.03	1.89	0.51	0.91	-0.23	0.44
	Shediac	-0.91	-0.30	-0.85	-1.26	2.46	0.96	0.53	0.38	-0.21	-0.12	-0.54	-0.13	0.40	1.24
	TESL		-0.54	-1.26	-0.82	-0.24	0.14	-0.21	0.46	2.61	0.40	-0.16	-0.36	-0.13	-0.15
	TSI		-0.65	-1.00	-1.37	0.04	-0.59	-0.88	1.89	1.05	0.62	0.20	0.70	0.17	-0.16
	TASO		-0.51	-0.90	-0.87	-0.48	-0.46	-0.53	2.42	1.19	0.38	-0.13	-0.09	-0.14	-0.02
	TIDM		-1.63	-1.23	-0.17	0.41	-0.48	-0.81	1.26	-0.28	1.34	0.89	0.71	1.10	1.13
	TCEN					2.24	-0.68	-0.96	-0.42	0.29	-0.04	0.13	-0.57	0.53	0.31
	TBB		-1.33	-1.22	-0.88	-0.50	1.59	-0.07	-0.46	0.19	1.40	0.91	0.38	1.34	0.79
	TDC		-0.12	-2.56	-0.33	0.41	0.80	0.37	0.63	-0.75	0.70	-0.10	0.95	1.41	-0.50
	wGSL		-0.66	-1.09	-1.12	-0.29	-0.44	-0.53	2.00	1.51	0.51	-0.02	0.14	-0.03	-0.12
	sGSL		-1.63	-1.23	-0.17	0.41	-0.48	-0.81	1.26	-0.28	1.34	0.89	0.71	1.10	1.13
	eGSL		-0.08	-2.46	-0.80	0.42	1.22	-0.08	-0.09	-0.15	1.10	0.51	0.40	1.64	0.32
Large calanoids	Rimouski							-0.22	-0.11	1.58	0.69	-0.83	-1.13	-0.10	-0.31
	Gaspé Current	-0.29	-0.50	-1.34	-0.12	1.95	-0.09	-0.95	0.09	0.92	0.31	1.27	-1.25	-1.04	0.21
	Anticosti Gyre	-0.93	-0.78	1.11	-1.51	1.77	1.36	0.39	0.20	-0.29	-0.64	-0.56	-0.13	-1.82	0.62
	Shediac	-0.38	0.03	-0.40	-0.85	2.59	0.82	0.37	0.38	-0.20	-0.30	-1.16	-0.90	-1.52	0.72
	TESL		0.30	-0.69	-0.03	-0.04	0.01	0.92	-0.21	2.26	0.09	-1.16	-1.44	-1.12	-0.72
	TSI		-0.25	0.14	-0.90	1.37	-0.36	-0.81	1.76	1.26	-0.64	-1.06	-0.51	-0.51	0.18
	TASO		-0.38	-0.48	-0.62	-0.18	-0.58	-0.18	2.64	1.13	-0.36	-0.51	-0.48	-0.81	0.11
	TIDM		-1.58	0.14	0.60	0.63	0.04	-0.99	0.92	0.62	1.52	-0.51	-1.39	-1.38	1.53
	TCEN					2.09	-0.41	-0.51	-0.52	0.54	-0.03	0.11	-1.28	-1.22	0.17
	TBB		-0.87	-0.53	-0.13	-0.43	1.61	-0.18	-1.68	0.95	1.54	-0.06	-0.21	-0.52	1.12
	TDC		1.68	-0.99	0.46	0.13	0.82	-0.96	0.33	0.80	-0.24	-0.15	-1.89	-0.86	0.06
	wGSL		-0.24	-0.41	-0.66	0.36	-0.48	-0.07	2.04	1.72	-0.39	-1.00	-0.87	-0.95	-0.11
	sGSL		-1.58	0.14	0.60	0.63	0.04	-0.99	0.92	0.62	1.52	-0.51	-1.39	-1.38	1.53
	eGSL		1.13	-1.35	-0.40	0.40	1.00	-0.69	-0.70	1.26	0.72	0.19	-1.57	-1.22	0.81
Cyclopoids	Rimouski							-0.84	-0.71	-0.31	-0.66	1.45	1.07	0.14	-0.52
	Gaspé Current	0.18	-0.66	-2.36	-0.37	0.01	1.15	0.26	-0.72	-0.36	1.09	0.92	0.86	0.80	-1.21
	Anticosti Gyre	0.60	-1.06	-1.98	0.03	-0.51	1.99	-0.63	-0.01	-0.04	0.29	0.77	0.56	1.07	-0.50
	Shediac	-1.29	-1.29	-1.19	1.07	-0.82	1.23	-0.27	0.41	0.98	1.31	-0.04	-0.09	0.81	0.66
	TESL		-0.66	-1.98	0.18	-0.33	2.01	0.38	-0.46	0.94	-0.10	0.35	-0.32	-0.89	-1.29
	TSI		0.43	-2.09	1.30	-0.75	1.10	-1.07	0.74	-0.04	-0.09	-0.02	0.49	-0.37	-1.14
	TASO		-0.46	-1.61	1.78	-0.59	0.98	-0.68	1.42	-0.45	-0.09	-0.18	-0.12	-0.48	-0.68
	TIDM		-0.76	-1.22	2.61	-0.34	0.39	-0.85	0.23	-0.08	0.23	-0.14	-0.07	-0.53	-0.11
	TCEN					1.91	0.76	-1.50	-0.42	-0.27	-0.44	-0.21	0.17	0.53	-0.17
	TBB		-0.35	-1.37	1.80	-0.16	1.91	-0.65	-0.62	-0.17	-0.12	0.17	-0.45	-0.08	-0.24
	TDC		-0.28	-1.77	2.23	-0.03	0.80	-0.98	0.06	-0.21	0.36	-0.13	-0.06	0.02	-0.75
	wGSL		-0.36	-2.09	1.37	-0.64	1.47	-0.64	0.80	0.10	-0.09	0.03	0.05	-0.61	-1.12
	sGSL		-0.76	-1.22	2.61	-0.34	0.39	-0.85	0.23	-0.08	0.23	-0.14	-0.07	-0.53	-0.11
	eGSL		-0.15	-1.59	2.20	0.10	1.24	-0.91	-0.35	-0.22	-0.04	-0.05	-0.23	0.03	-0.43
Copepod: warm species	Rimouski							-1.04	-0.91	1.41	-0.13	-0.32	0.99	8.25	0.32
	Gaspé Current	-0.72	0.39	-1.06	-0.99	-0.43	-0.66	-0.78	-0.49	0.86	1.86	0.48	1.53	6.02	3.06
	Anticosti Gyre	-0.74	0.01	-0.86	-0.73	-0.71	0.02	-0.78	-0.53	0.73	2.05	1.74	-0.20	9.07	-0.18
	Shediac	1.97	0.52	1.83	0.31	-0.36	-0.40	-0.29	-0.73	-1.21	-0.32	-0.86	-0.46	-0.99	0.35
	TESL		0.37	-0.90	-0.90	-0.90	-0.78	1.58	-0.61	1.66	0.07	-0.55	0.95	2.30	0.97
	TSI		0.29	-0.97	-0.97	-0.97	-0.71	-0.76	-0.42	0.87	1.73	1.29	0.63	1.87	0.41
	TASO		-0.46	-0.89	-0.81	-0.73	-0.81	-0.89	-0.17	0.64	1.71	0.95	1.46	3.24	1.05
	TIDM		-0.43	-0.57	-0.57	-0.42	-0.57	-0.51	-0.07	-0.45	-0.01	2.72	0.89	1.11	6.75
	TCEN					-0.69	-0.65	-0.54	2.31	-0.38	-0.39	0.41	-0.06	6.33	4.14
	TBB		0.11	-0.81	-0.84	-0.77	-0.64	1.99	-0.23	-0.67	1.58	0.71	-0.42	2.63	9.35
	TDC		0.24	-1.04	-0.82	-0.83	-1.01	0.51	0.08	-0.34	0.89	2.30	0.03	3.37	3.23
	wGSL		-0.09	-0.99	-0.96	-0.92	-0.82	-0.63	-0.36	0.99	1.66	1.02	1.12	2.73	0.79
	sGSL		-0.43	-0.57	-0.57	-0.42	-0.57	-0.51	-0.07	-0.45	-0.01	2.72	0.89	1.11	6.75
	eGSL		0.73	-1.11	-0.95	-0.96	-1.05	0.84	0.64	-0.57	0.89	1.74	-0.20	4.75	6.14
Copepod: cold species	Rimouski							-0.97	-1.00	0.28	-0.54	0.83	1.41	5.45	1.43
	Gaspé Current	-0.91	-0.91	-0.84	-0.84	-0.84	0.16	0.38	-0.16	-0.13	0.43	1.59	2.07	4.80	1.10
	Anticosti Gyre	-0.67	-0.68	-0.96	-0.93	-0.84	-0.45	-0.45	0.33	0.11	1.93	1.21	1.38	2.21	-0.54
	Shediac	-0.76	-0.66	-0.75	-0.94	-0.80	-0.25	-0.03	-0.09	0.10	2.54	0.76	0.89	0.93	-0.16
	TESL		-0.67	-1.22	-0.95	-1.06	-0.23	-0.65	1.39	0.92	1.51	0.36	0.62	1.11	-0.33
	TSI		-1.22	-1.40	-1.14	-0.56	1.31	0.05	0.09	-0.08	1.09	1.29	0.59	1.95	0.68
	TASO		-2.59	-2.59	-2.59	1.58	-1.05	-1.23	-0.02	-0.42	-0.25	0.11	1.28	4.30	0.97
	TIDM		-0.68	-2.11	-0.55	0.36	0.36	0.68	0.48	-0.87	0.72	0.00	1.60	1.75	-0.40
	TCEN					-0.97	0.42	-0.57	1.14	0.97	-0.06	1.04	1.21	1.00	0.36
	TBB		-1.16	-1.42	-0.47	0.19	-0.59	-0.51	1.07	-0.61	0.88	1.22	1.40	1.84	0.68
	TDC		-0.78	-1.08	-0.97	-1.10	-0.51	-0.50	1.03	0.34	1.22	0.96	1.40	0.65	-0.49
	wGSL		-0.52	-2.26	-0.85	0.24	0.82	0.32	0.25	-0.65	0.84	0.57	1.24	2.54	0.17
	sGSL		-1.16	-1.42	-0.47	0.19	-0.59	-0.51	1.07	-0.61	0.88	1.22	1.40	1.84	0.68
	eGSL		-0.74	-1.23	-1.10	-1.12	-0.24	-0.53	1.22	0.66	1.10	0.81	1.16	0.90	-0.29

Figure 33. Normalized annual anomalies (scorecard) for six categories of zooplankton assemblages. Blue colours indicate anomalies below the mean and reds are anomalies above the mean.